Article

Immunity

MicroRNA-221 and -222 modulate intestinal inflammatory Th17 cell response as negative feedback regulators downstream of interleukin-23

Graphical abstract

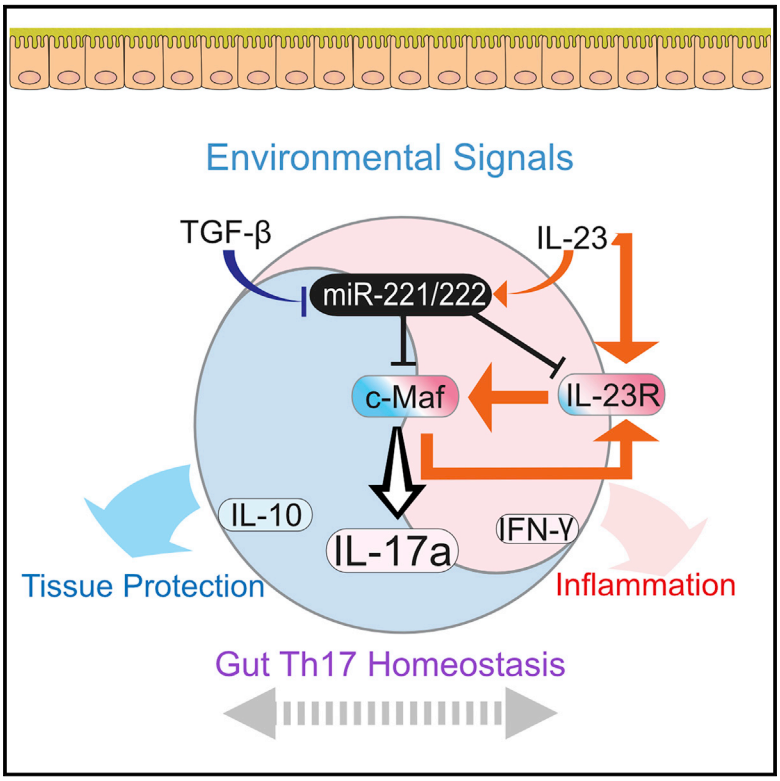

Highlights

- miR-221/222 are induced by proinflammatory cytokines and repressed by TGF-β
- Intestinal Th17 homeostasis is maintained without miR-221/222 in healthy hosts
- miR-221/222 target *Maf* and *Il23r* to constrain IL-23-induced Th17 cell response
- T cell-dependent miR-221/222 are protective against DSS-induced mucosal damage

Authors

Yohei Mikami, Rachael L. Philips, Giuseppe Sciumè, ..., Markus Hafner, Yuka Kanno, John J. O'Shea

Correspondence

kannoy@mail.nih.gov (Y.K.), john.oshea@nih.gov (J.J.O.)

In brief

Mikami et al. examine the role of miR-221/222 in helper T cells in the gut. MiR-221/222 are induced by IL-23 and suppressed by TGFβ, targeting *Maf* and *IL23r* for degradation. During inflammation, these miRNAs serve as a negative feedback rheostat to constrain IL23-Th17 cell responses.

Mikami et al., 2021, Immunity *54*, 514–525
March 9, 2021 Published by Elsevier Inc.
https://doi.org/10.1016/j.immuni.2021.02.015

CellPress

CellPress

Immunity

Article

MicroRNA-221 and -222 modulate intestinal inflammatory Th17 cell response as negative feedback regulators downstream of interleukin-23

Yohei Mikami,[1,6] Rachael L. Philips,[1,2] Giuseppe Sciumè,[1,7] Franziska Petermann,[1,9] Françoise Meylan,[1,14] Hiroyuki Nagashima,[1] Chen Yao,[1] Fred P. Davis,[1,8] Stephen R. Brooks,[3] Hong-Wei Sun,[3] Hayato Takahashi,[1,10] Amanda C. Poholek,[1,11] Han-Yu Shih,[1,12] Behdad Afzali,[1,13] Stefan A. Muljo,[4] Markus Hafner,[5] Yuka Kanno,[1,*] and John J. O'Shea[1,15,*]

[1]Molecular Immunology and Inflammation Branch, National Institute of Arthritis and Musculoskeletal and Skin Diseases, National Institutes of Health, Bethesda, MD 20892, USA

[2]Postdoctoral Research Associate Program, National Institute of General Medical Sciences, National Institutes of Health, Bethesda, MD 20892, USA

[3]Biodata Mining and Discovery Section, National Institute of Arthritis and Musculoskeletal and Skin Diseases, National Institutes of Health, Bethesda, MD 20892, USA

[4]Laboratory of Immune System Biology, National Institute of Allergy and Infectious Diseases, National Institutes of Health, Bethesda, MD 20892, USA

[5]RNA Molecular Biology Group, National Institute of Arthritis and Musculoskeletal and Skin Diseases, National Institutes of Health, Bethesda, MD 20892, USA

[6]Present address: Division of Gastroenterology and Hepatology, Department of Internal Medicine, Keio University School of Medicine, Tokyo 160-8582, Japan

[7]Present address: Department of Molecular Medicine, Sapienza University of Rome, Roma 00185, Italy

[8]Present address: Celsius Therapeutics, Cambridge, MA 02139, U.S.A

[9]Present address: German Cancer Research Center, Heidelberg 69120, Germany

[10]Present address: Department of Dermatology, Keio University, Tokyo 160-8582, Japan

[11]Present address: Division of Pediatric Rheumatology, Department of Pediatrics, University of Pittsburgh School of Medicine, Pittsburgh, PA 15260, U.S.A

[12]Present address: Neuro-Immune Regulome Unit, National Eye Institute, National Institutes of Health, Bethesda MD 20892, U.S.A

[13]Present address: Immunoregulation Section, National Institute of Diabetes and Digestive and Kidney Diseases, National Institutes of Health, Bethesda MD 20892, U.S.A

[14]Present address: Translational Immunology Section, National Institute of Arthritis and Musculoskeletal and Skin Diseases, National Institutes of Health, Bethesda MD 20892, U.S.A

[15]Lead contact

*Correspondence: kannoy@mail.nih.gov (Y.K.), john.oshea@nih.gov (J.J.O.)

https://doi.org/10.1016/j.immuni.2021.02.015

SUMMARY

MicroRNAs are important regulators of immune responses. Here, we show miR-221 and miR-222 modulate the intestinal Th17 cell response. Expression of miR-221 and miR-222 was induced by proinflammatory cytokines and repressed by the cytokine TGF-β. Molecular targets of miR-221 and miR-222 included *Maf* and *Il23r*, and loss of miR-221 and miR-222 expression shifted the transcriptomic spectrum of intestinal Th17 cells to a proinflammatory signature. Although the loss of miR-221 and miR-222 was tolerated for maintaining intestinal Th17 cell homeostasis in healthy mice, Th17 cells lacking miR-221 and miR-222 expanded more efficiently in response to IL-23. Both global and T cell-specific deletion of miR-221 and miR-222 rendered mice prone to mucosal barrier damage. Collectively, these findings demonstrate that miR-221 and miR-222 are an integral part of intestinal Th17 cell response that are induced after IL-23 stimulation to constrain the magnitude of proinflammatory response.

INTRODUCTION

Helper T (Th) cells play a major role in immunoregulation, host defense, and autoimmune pathogenesis by differentiating into specialized subsets with distinct functionalities (Zhu et al., 2010). Major Th subsets include T effector cells that produce specialized cytokines (Th1, Th2, Th17), regulatory T (Treg) cells that suppress T effectors, and follicular B helper T (Tfh) cells that interact with and facilitate B cell differentiation (O'Shea and Paul, 2010). At intestinal mucosal barriers at which commensal bacteria reside, resident

cells and commensal bacteria constantly interact and communicate not only physically but also through soluble factors such as cytokines (Ivanov et al., 2009; Omenetti et al., 2019). In particular, interleukin-17 (IL-17) producing Th17 cells provide a unique and important role in preserving immune homeostasis in the gut (Korn et al., 2009; Littman and Rudensky, 2010).

Multiple cytokines and transcription factors take part in the generation of Th17 cells. Th17 cell-instructive cytokines include IL-6, IL-21, and IL-23, which mainly act via the transcription factor STAT3 alongside other STATs (Langrish et al., 2005; Yang et al., 2007). Transforming growth factor-β (TGF-β) coupled with IL-6 supports *in vitro* differentiation of IL-17-producing cells, whereas other multi-cytokine combinations, such as IL-23, IL-6, and IL-1β in the absence of TGF-β, promote Th17 cells with prominent inflammation signature (Bettelli et al., 2006; Esplugues et al., 2011; Gaublomme et al., 2015; Ghoreschi et al., 2010; Lee et al., 2012). Thus, the diverse combinatorial cytokine milieu *in vivo* is likely to instruct a spectrum of Th17 cells in tissues (Stockinger and Omenetti, 2017).

Cytokine signaling subsequently initiates intracellular transcription factor networks that further drive the Th17 cell program, including the lineage-determining transcription factor RORγt (Ivanov et al., 2006), which coordinates with IRF4 (Schraml et al., 2009), BATF (Schraml et al., 2009), AHR (Quintana et al., 2008; Veldhoen et al., 2008), c-Maf (Rutz et al., 2011; Tanaka et al., 2014), and other factors (Ciofani et al., 2012; Yosef et al., 2013). The phenotypic outcome of Th17 cell differentiation driven by combination of multiple transcription factors represents an additional aspect of heterogeneity in gene expression profiles. In particular, the degree to which inflammatory signature manifests is relevant to understanding the physiology of intestinal mucosal immunity at healthy steady state as well as pathological autoimmune conditions (Gaffen et al., 2014; Patel and Kuchroo, 2015; Stockinger and Omenetti, 2017). Furthermore, post-transcriptional regulators are likely to impact the heterogeneity of Th17 cells. We hypothesize that microRNAs (miRNAs) with selective expression in different Th17 cell conditions might play such regulatory roles.

Named after their small size of around 21–25 nucleotides, miRNAs are non-coding RNAs that negatively regulate gene expression in a target sequence-specific manner at the post-transcriptional level (Bartel, 2018). Depending on the degree of complementarity between a miRNA and its target, a miRNA can target multiple mRNAs to influence diverse arrays of developmental and physiological processes, including Th cell differentiation (Baumjohann and Ansel, 2013). By conducting unbiased expression analysis of miRNAs across immune cells, we have reported distinct miRNA signatures of various immune cells (Kuchen et al., 2010), in which expression of miR-221 and miR-222, two miRNAs presumed to be generated from a single pri-miRNA transcript, was detected in subsets of innate and adaptive lymphocytes. Recently, miR-221 and miR-222 were reported to play a role in macrophages to induce lipopolysaccharide (LPS) tolerization by silencing inflammatory genes (Seeley et al., 2018). In contrast, the cell intrinsic function of miR-221 and miR-222 in adaptive cells such as Th cells has not been fully investigated.

In this study, we examined the functional roles of miR-221 and miR-222 in T cells in mice in which these miRNAs were deleted globally and in a T cell-specific manner. We found that a notable phenotype in these mice was related to response of Th17 cell populations in the gut in inflammatory conditions. miR-221 and miR-222 targeted *Maf* and *Il23r* to control Th17 cell populations and limited the expansion of IL-17$^+$ RORγt$^+$ cell population in response to IL-23. Upon intestinal barrier perturbation with dextran sodium sulfate (DSS), T cell-specific loss of miR-221 and miR-222 was associated with exacerbated damage. Beyond the impact on innate immune cells, our observations collectively support an important role of miR-221 and miR-222 in regulating intestinal Th17 cells and indicate that miR-221 and miR-222 act as negative feedback regulators downstream of IL-23 to modulate the magnitude of intestinal Th17 cell response in inflammatory milieu.

RESULTS

Transcriptional regulation of miR-221 and miR-222 in CD4$^+$ T cells

Using previously reported global miRNA expression profiling (Kuchen et al., 2010), miR-221 and miR-222 were found to be expressed dynamically among various blood cells (Figure S1A). Focusing on CD4$^+$ Th cell subsets, miR-221 and miR-222 expression was noted to be high in Th1, Th17, and Tfh cells and low in Th2 and Treg cells, suggesting that miR-221 and miR-222 expression is differentially regulated by diverse cytokine signals. To test this, epigenetic histone marks at the *Mir221* and *Mir222* genomic loci and miR-221 and miR-222 expression were examined in *in vitro* differentiated Th1 and Th17 cells; Th1 cells were differentiated with IL-12, and Th17 cells were differentiated under TGF-β or IL-23 conditions (see experimental procedures for details). Examination of the chromatin landscape in Th1 and Th17 cells revealed multiple enhancer activities upstream of the *Mir221 and Mir222* loci marked by p300, H3K4me1, and H3K4me3 (Figure 1A). These regions were highly conserved across mammalian species (Figure S1B) and overlapped with regions identified as super-enhancer loci in human T cells (Figure S1C). Under Th1 conditions, p300-prominent enhancers were also positive for STAT4 binding (Figure 1A), the predominant STAT protein preferentially activated by IL-12 (Kaplan et al., 1996). In the absence of STAT4, active chromatin marks and miR-221 and miR-222 expression were reduced (Figures 1A and 1B), indicating a positive regulatory role for STAT4 driving miR-221 and miR-222 expression in Th1 cells. Similarly, STAT3 binding overlapped with active enhancer marks in Th17 cells from both cytokine conditions (Figure 1A) (Ghoreschi et al., 2010), and both enhancer activity and miR-221 and miR-222 expression were decreased when STAT3 was absent (Figure 1C; Figure S1D). Therefore, miR-221 and miR-222 expression is apparently controlled by STAT proteins at an extended regulatory region in Th1 and Th17 lymphocytes.

Additionally, gene expression and histone epigenetic marks suggest that TGF-β negatively regulates miR-221 and miR-222 expression. The presence of TGF-β in the Th17 polarization cocktail substantially enhanced deposition of repressive H3K27me3 marks (Figure 1A). This is consistent with expression data demonstrating that miR-221 and miR-222 are induced in Th17 cells generated by IL-23 but not TGF-β conditions (Figure S2B); this differential response of miR-221 and miR-222 to IL-23 versus TGF-β will be further addressed below. Furthermore, miR-221

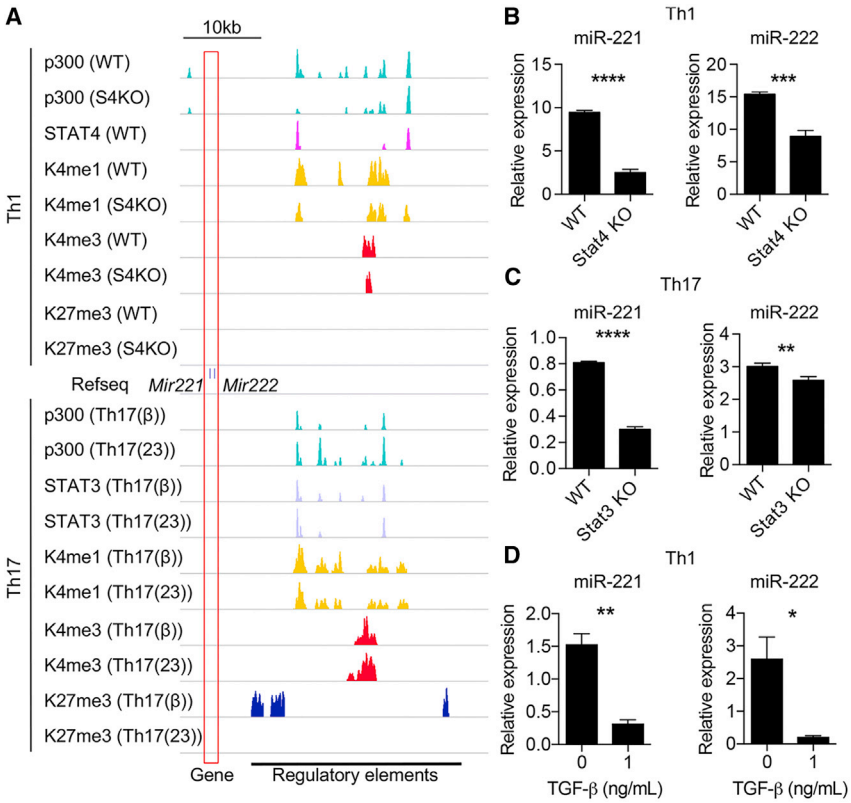

Figure 1. Regulation of miR-221 and miR-222 expression in Th1 and Th17 cells

(A) Chromatin landscape of the extended *Mir221* and *Mir222* locus (boxed in red) in Th1 cells (above *Mir221* and *Mir222* gene track) and Th17 cells (below *Mir221* and *Mir222* track). For Th1 condition, wild-type (WT) and STAT4 deficient (S4KO) cells were evaluated. For Th17 condition, TGF-β (TGF-β+IL-6) and IL-23 (IL-6+IL-23) conditions were used with WT cells. Chromatin immunoprecipitation sequencing (ChIP-seq) for binding of p300, STAT4, STAT3, H3K4me1, H3K4me3, and H3K27me3 is shown (Table S1; data are derived from GSE40463, Vahedi et al., 2012; GSE22104, Wei et al., 2010; GSE23681, Ghoreschi et al., 2010; and GSE65621, Hirahara et al., 2015). Putative regulatory regions with enhancer activity are marked at the bottom.

(B–D) Quantitative reserve transcription polymerase chain reaction (RT-qPCR) analysis of miR-221- and miR-222-3p expression in Th1 conditions comparing WT and S4KO (B), Th17-full conditions (TGF-β, IL-23, and others; see STAR methods) comparing WT and S3KO (C), and Th1 conditions ± TGF-β (D). (*$p < 0.05$, **$p < 0.01$, ***$p < 0.005$, ****$p < 0.001$; Student's t test) Data are representative of at least two independent experiments. Data are shown as means with SD. See also Figure S1.

and miR-222 expression was downregulated when TGF-β was added to Th1 cultures (Figure 1D). Collectively, our data demonstrate that miR-221 and miR-222 expression is induced by proinflammatory cytokines and repressed by TGF-β.

Effect of *Mir221* and *Mir222* deletion on T cell development and *in vitro* Th differentiation

We first examined the function of miR-221 and miR-222 in lymphocytes using germline *Mir221 and Mir222* gene-deletion mice. We aimed for simultaneous deletions of juxtaposing *Mir221 and Mir222* loci via a pair of flox sites and generated *Mir221Mir222*$^{fl/fl}$ mice (flox allele in Figure S2A). Subsequently *Mir221Mir222* $^{fl/fl}$ mice (denoted as wild-type [WT] hereafter) were crossed to *Pgk1*-cre mice to create germline deletion of both *Mir221* and *Mir222* (designated miR-221/222-knockout [KO] mice) (KO allele in Figure S2A). miR-221/222-KO mice were fertile and developed normally. miRNA sequencing (miRNA-seq) of various *in vitro*-generated Th lineages confirmed that miR-221 and miR-222 were successfully deleted (Figures S2B and S2C). Specifically, the expression of miR-221/222-3p (from the 3′-arms of the precursor miRNA) in WT cells was high in Th1 and IL-23-treated Th17 cells and low in TGF-β-treated Th17 and induced Treg (iTreg) cells (Figure S2B). Because miRNAs may regulate other miRNAs, we sought to determine whether deletion of miR-221 and miR-222 would impact miRNAs relevant to T cells. Importantly, deleting the *Mir221 and Mir222* loci did not alter expression of other miRNAs when evaluated globally (Figure S2C) or specifically (iTreg-specific miR-10a; Figure S2D) (Takahashi et al., 2012).

To determine potential developmental effects of miR-221 and miR-222 deletion, we examined T populations in the thymus and spleen in miR-221/222-KO mice. While the proportions of specific thymocyte subsets were slightly altered in KO mice, the populations of lymphocytes in the spleen remained unchanged (Figures 2A–2D), indicating that miR-221 and miR-222 deletion does not dramatically alter T cell development or the composition of splenic lymphocytes. Next, *in vitro* Th differentiation of naive cells derived from secondary lymphoid tissues was evaluated comparing WT and miR-221/222 KO cells. When cell proliferation was measured by carboxyfluorescein diacetate succinimidyl ester (CFSE) dilution, a slight impairment was detected for miR-221/222-KO cells in Th null condition (Figures S2E and S2F). Under Th1 conditions, the production of interferon γ (IFN-γ) as well as the expression of T-bet was decreased in miR-221/222-KO CD4$^+$ T cells (Figure 2E). In contrast, the proportion of Th17 cells, generated under full cocktail conditions (see STAR methods), was significantly increased in miR-221/222-KO CD4$^+$ T cells, as assessed by IL-17 production and RORγt expression (Figure 2F). Interestingly, the observed difference in IL-17 production was not due to differences in gut microbiome among mice, as microbiome profiles were variable but comparable between WT and miR-221/222 KO mice (Figure S2G). Collectively, our data indicate that deletion of miR-221 and miR-222 allows for normal development of lymphocytes but differentially impacts *in vitro* CD4$^+$ Th differentiation of Th1 and Th17 subtypes.

Loss of miR-221 and miR-222 enhances activation-dependent IL-17 production in intestinal CD4$^+$ T cells

To determine the impact of miR-221 and miR-222 on CD4$^+$ Th subsets *in vivo*, CD4$^+$ Th subsets in small intestine lamina propria

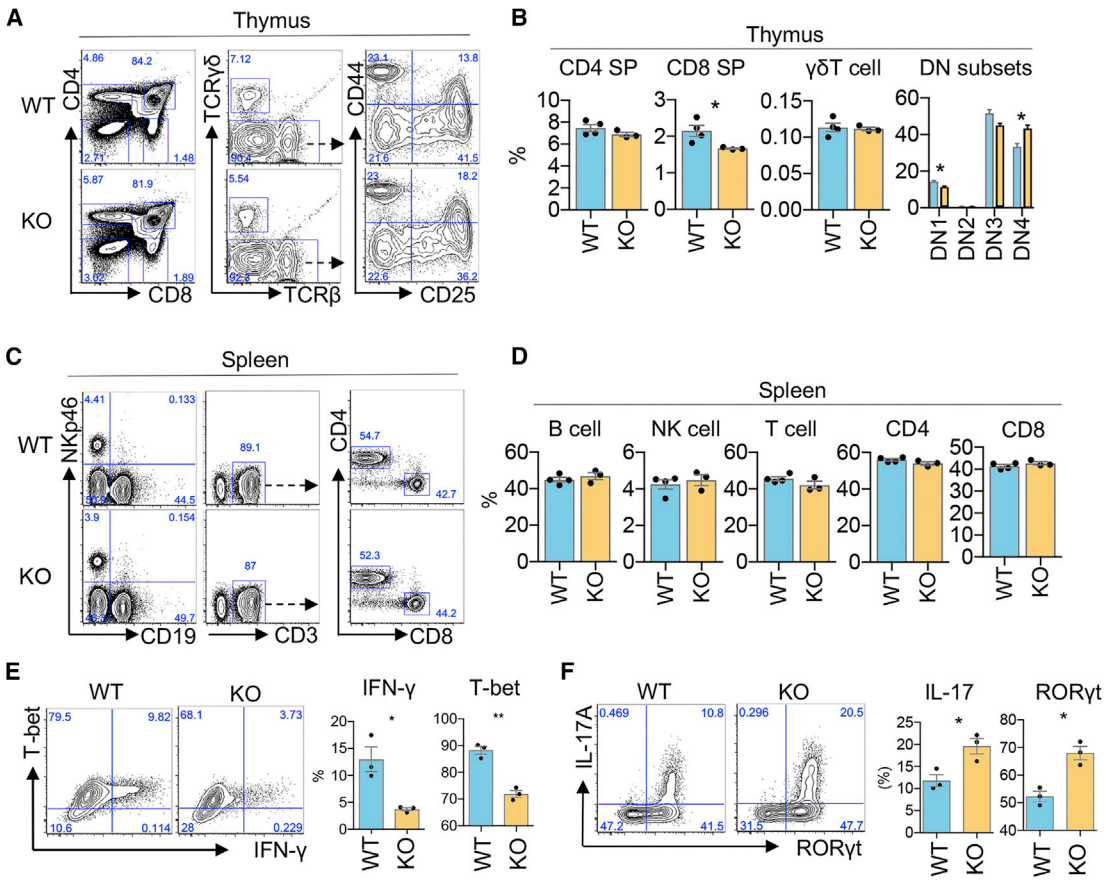

Figure 2. Effect of miR-221 and miR-222 deletion on T cell development and *in vitro* Th differentiation

(A and B) Flow cytometric analyses comparing WT and miR-221/222 KO thymocyte subsets. Plots show the frequency of CD4SP and CD8SP cells, γδT cells (from CD4−CD8− gate), and DN subsets (from CD4−CD8− TCRγδ− gate). CD25 and CD44 distinguish DN subsets (DN1: CD25−CD44+; DN2: CD25+CD44+; DN3: CD25+CD44−; DN4 CD25−CD44−). Plots depict mean with SEM, with 3–4 mice/group (*$p < 0.05$; Student's t test).

(C and D) Flow cytometric analyses comparing WT and miR-221/222 KO splenocytes: B cells (NKp46− CD19+), NK cells (NKp46+ CD19−), αβT cells (TCRβ+ NKp46− CD19−), and $CD4^+$ and $CD8^+$ T cells.

(E) Naive $CD4^+$ T cells of indicated genotypes were cultured under Th1 condition for 3 days. Flow cytometric analysis of cells expressing IFN-γ and T-bet are shown. The left panel shows a representative result from biological triplicates with cumulative data shown on the right (*$p < 0.05$,**$p < 0.01$; Student's t test). Data are represented as mean with SEM. Data are representative of at least three independent experiments.

(F) Naive $CD4^+$ T cells of indicated genotypes were cultured under Th17-full conditions for 3 days. Flow cytometric analysis of cells expressing IL-17A and RORγt are shown. Panels show a representative result from biological triplicates with cumulative data shown in plots (*$p < 0.05$; Student's t test). Data are represented as mean with SEM.

See also Figure S2.

lymphocytes (LPLs) were examined in co-housed miR-221/222-KO and WT mice. Using flow cytometry to identify subsets based on transcription factor expression (Figure 3A), there was no significant difference in the frequency of $CD4^+$ Th subsets (Figure 3B), but the number of Treg and Th1 lymphocytes were reduced in miR-221/222 mice compared to WT mice (Figure 3C). Since $CD4^+$ Th subsets are also identified by cytokine production, intestinal lymphocytes were stimulated with phorbol myristate acetate (PMA) and ionomycin *ex vivo* to measure IFN-γ and IL-17A production. While there was no difference in the frequency of IFN-γ^+ lymphocytes between mice, miR-221/222-deficient $CD4^+$ T cells exhibited an increase in the proportion of IL-$17A^+$ cells compared to WT mice (Figure 3D). Furthermore, the frequency of RORγt^+ IL-$17A^+$ $CD4^+$ T cells was increased in miR-221/222-KO mice with no difference in the frequency of RORγt^+ cells (Figure 3E), suggesting that miR-221 and miR-222 are required to constrain IL-17A production upon activation. Of note, IL-17^+ cells from miR-221/222-KO mice also had higher levels of IL-17 protein on a per cell basis compared to WT cells, as measured by mean fluorescence intensity (MFI) (Figure 3E). Collectively, our data indicate that deletion of miR-221 and miR-222 impacts activation-dependent cytokine production of peripheral Th17 cells derived from the gut.

To obtain a clearer picture of the impact of miR-221 and miR-222 deletion on unperturbed tissue-resident IL-17-producing $CD4^+$ T cells, healthy IL-17-GFP reporter mice (IL17-GFP-WT and IL17-GFP-miR-221/222-KO) were used to isolate intestinal IL-17-GFP^+ $CD4^+$ cells (Figure S3A) for single-cell RNA-seq analysis. Comparable numbers of *Il17-gfp*$^+$ $CD4^+$ cells were captured from WT and miR-221/222-KO mice (WT: 688 cells;

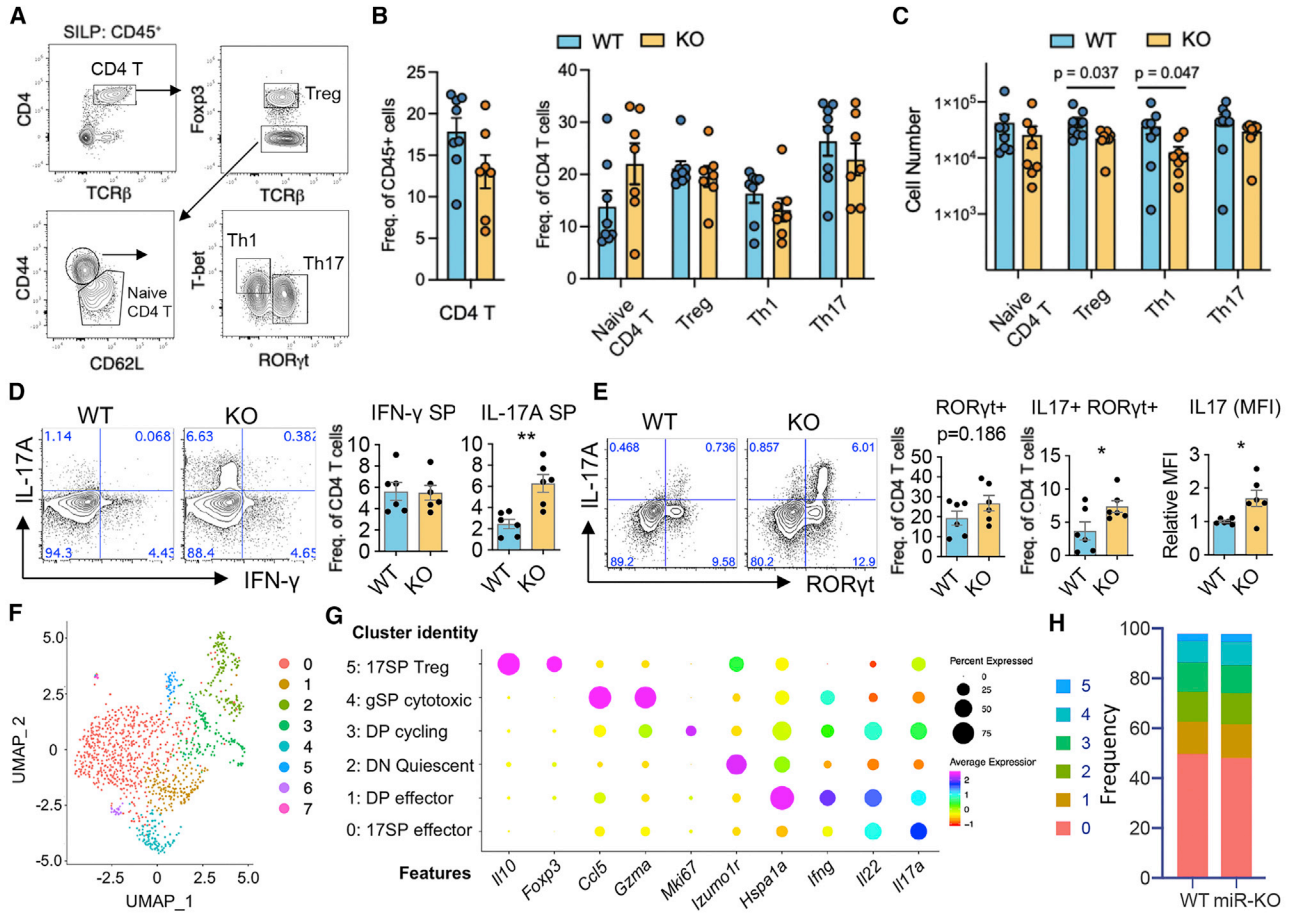

Figure 3. Loss of miR-221 and miR-222 enhances IL-17 production in activated intestinal CD4⁺ T cells

(A–E) Lymphocytes were isolated from the small intestine of healthy WT and miR-221/222-KO mice and analyzed by FACS.

(A) Representative FACS plots show Th subsets defined as naive, Treg, Th1, and Th17.

(B and C) Pooled data comparing the frequencies (B) and cell number (C) of Th subsets between WT (n = 8) and miR-221/222-KO (n = 7) according to (A).

(D) Proportion of CD4⁺ T cells expressing IL-17A and IFN-γ following PMA-I stimulation.

(E) Proportion of CD4⁺ T cells expressing RORγt and IL-17A after PMA-I stimulation.

(B–E) Data are represented as mean with SEM. Plots are pooled from 6–8 mice/group from at least three independent experiments. (*p < 0.05,**p < 0.01; Student's t test)

(F–H) *Il17-gfp*+ cells from the small intestine of healthy WT and miR-221/222-KO mice were used for single-cell RNA sequencing (see Figure S3A for gating strategy).

(F) UMAP plot depicts eight clusters separated in an unbiased manner. Custers 6 and 7 contained less than 10 cells of unknown origin and were removed from further analysis.

(G) Dot plot shows the expression of representative marker genes to define cluster identities.

(H) Stacked bar plots depict the frequency of each cluster between WT and miR-221/222-KO mice.

KO: 526 cells). Differential gene expression resolved eight clusters, two of which represent minor cell contamination of unknown origin and thus were excluded from further analysis (clusters 6–7; Figure 3F). While all cells were captured based on the presence of "proxy" GFP protein that was driven by endogenous *Il17a* gene promoter, there were considerable differences in endogenous *Il17a* transcript expression among individual cells, as well as other key phenotype-defining transcripts (Figures 3G and 3H). We identified cells expressing predominantly *Il17a* and *Il22* (17 single-positive [SP] effector); both *Il17a and Ifng* (double-positive [DP] effector); quiescent cells with minimal cytokine expression (double-negative (DN) quiescent); actively cycling cells expressing *Mki67*, *Il17a*, and *Ifng* (DP cycling); cells expressing *Ifng*, *Gzma*, *Hspa1a*, and *Ccl5* (gSP cytotoxic); and cells expressing *Il17a* along with *Il10* and *Foxp3* (17SP Treg) (Figure 3G). The frequencies of each Th17 cell subset (clusters 0–5) were comparable between WT and miR-221/222-KO samples (Figure 3H), indicating that the overall balance of heterogeneity among intestinal Th17 cells is maintained in the absence of miR-221 and miR-222 in healthy mice.

Collectively, our findings indicate an interesting dichotomy regarding the phenotype of intestinal Th17 cells from miR-221/222 KO mice. Whereas loss of miR-221 and miR-222 was tolerated in healthy, unperturbed mice and intestinal Th17 cell homeostasis was maintained, intestinal Th17 cells devoid of miR-221 and miR-222 produced more IL-17A upon activation.

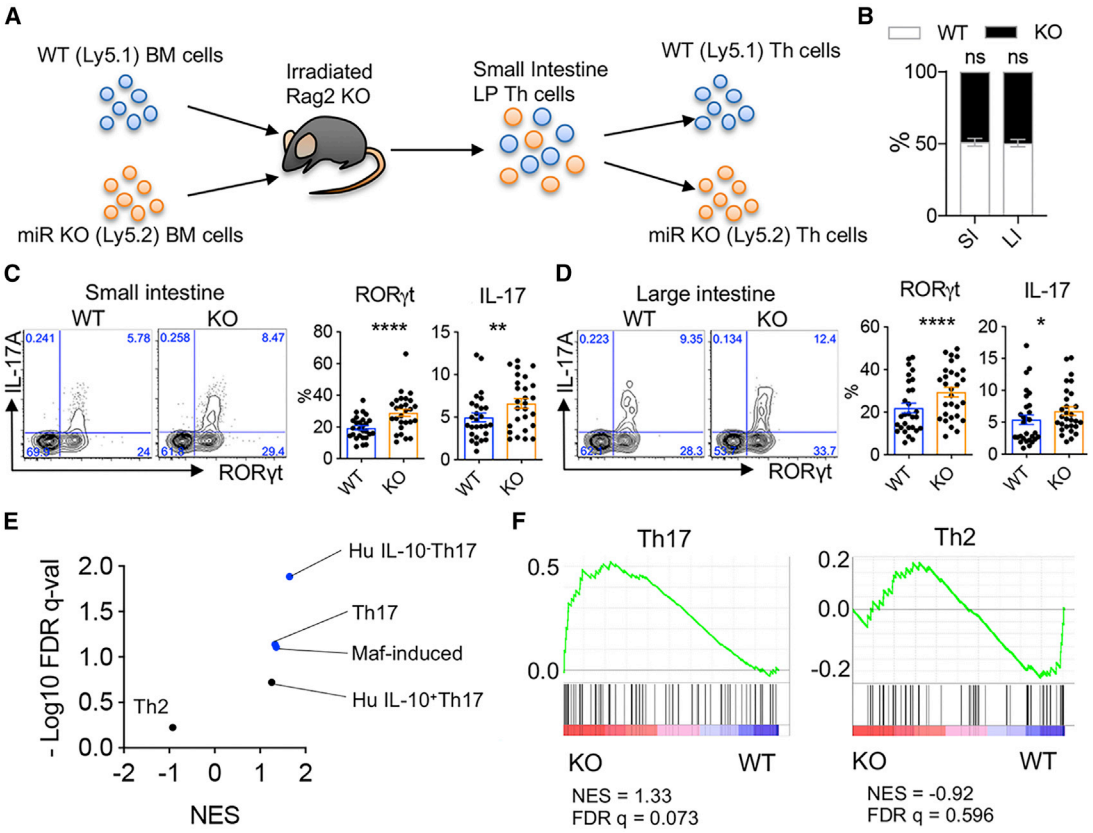

Figure 4. miR-221/222-deficient Th17 cells exhibit a cell intrinsic proinflammatory Th17 transcriptomic signature

(A) Diagram of mixed bone marrow (BM) chimera experiment using congenic WT and miR-221/222-KO BM cells. Irradiated *Rag2*-KO hosts were reconstituted with 1:1 ratio of WT (CD45.1) and miR-221/222-KO (CD45.2) BM. Th cells populating the gut were analyzed at 7–8 weeks post BM transfer and identified by congenic markers.

(B–F) Chimerism (B) and proportions of Th cells expressing IL-17 and RORγt from the small intestine (C) or large intestine (D) are depicted. Plots represent mean with SEM of pooled samples isolated from 27 mice (small intestine) and 29 mice (large intestine) from two independent experiments.

(E–F) $CD4^+$ T cells isolated from the small intestine of BM chimera mice were separated into WT and miR-221/222-KO fractions and mRNA-seq was performed.

(E) Summary of 5 GSEA (Broad Institute) analyses for signature genes of Th cell subsets. Signature gene sets were extracted from published data. Also see Table S2.

(F) GSEA plots for signature genes of Th17 and Th2 subsets. Replicates were compared for significance, ns (not significant), *$p < 0.05$, **$p < 0.01$, and ****$p < 0.001$. See also Figure S4.

Therefore, miR-221 and miR-222 may regulate the Th17 cell response under certain cellular environments that occur upon pathological provocation.

miR-221/222-deficient Th17 cells exhibit a cell intrinsic proinflammatory Th17 transcriptomic signature

As a variety of intrinsic and extrinsic factors may influence Th17 cells in the gut, mixed bone marrow (BM) chimera mice were first used to test the cell intrinsic roles of miR-221 and miR-222. Irradiated *Rag2*$^{-/-}$ mice were reconstituted with BM obtained from miR-221/222-KO and WT congenic mice at a 1:1 ratio (Figure 4A). After 6 to 7 weeks following BM reconstitution, $CD4^+$ T cells were isolated from the small and large intestine lamina propria and congenic markers were used to evaluate WT and KO cells separately. The absence of miR-221 and miR-222 had no significant impact on lymphopoiesis, as co-transferred WT and miR-221/222-KO T cells populated gut mucosal tissues similarly (Figure 4B). While stem cell transplantation in the setting of lymphopenia provokes inflammatory responses, cells are exposed to the same local microenvironment. In this setting, we noted the presence of more IL-17-producing Th17 cells from miR-221/222-KO fractions compared to WT fractions in the small intestine and large intestine (Figures 4C and 4D). Therefore, loss of miR-221 and miR-222 resulted in more gut IL-17-producing cells in a cell intrinsic manner.

Next, mRNA-seq was used to determine the transcriptomic signature of WT and miR-221/222-deficient $CD4^+$ T cells from BM-reconstituted mice (n = 3; Figures 4A; Figure S4). With a cut-off of 1.5-fold change and a p value of <0.05, 28 genes were found to be differentially regulated between WT and KO cells (Figure S4). In order to further assess differential gene expression in "bulk" $CD4^+$ T cell samples, gene lists were generated from multiple publicly available datasets to perform gene set enrichment analysis (GSEA). These datasets utilized include (1) Th17 genes (Ciofani et al., 2012), (2) IL-10-positive Th17 genes, (3) IL-10-negative Th17 genes (Aschenbrenner et al., 2018),

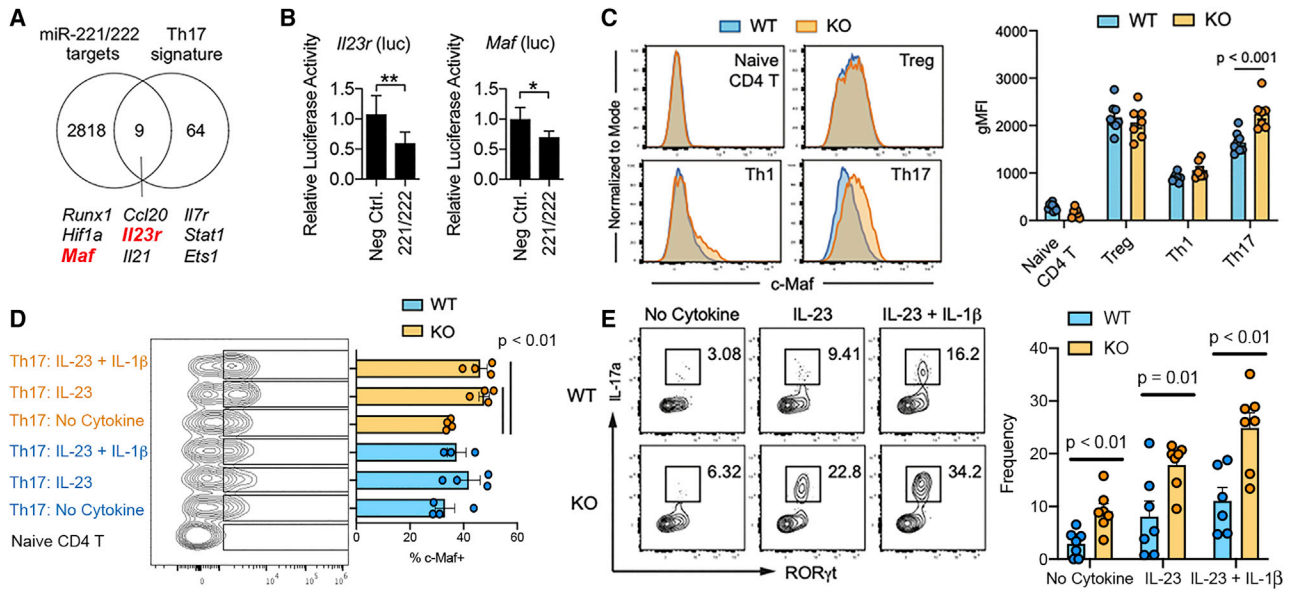

Figure 5. miR-221 and miR-222 target *Maf* and *Il23r* to regulate Th17 response

(A) Overlap of curated Th17-signature genes (Ciofani et al., 2012) and predicted target genes for miR-221 and miR-222 (microRNA.org: Betel et al., 2008).

(B) HEK293 cells were transfected with luciferase reporter fused to 3′ UTR of *Il23r* or *Maf* together with miR-221 plus miR-222 or control miRNA (random sequences). Luciferase activity was evaluated at 24 h post-transfection. Data are representative of two independent experiments.

(C) Flow cytometric analysis of c-Maf in WT and miR-221/222-KO Th cells, gated according to Figure 3A. Data show representative flow cytometry plots and the pooled data as mean with SEM and statistical evaluation (Student's t test).

(D and E) *Ex vivo* intestinal lymphocytes were stimulated *in vitro* with IL-23 or IL-23 and IL-1β for 6 h and subjected to flow cytometric analysis to measure the induction of c-Maf expression in Th17 cells (D; 3–4 mice/group) and the frequency of IL-17-producing RORγt$^+$ CD4$^+$ T cells in WT and miR-221/222-KO mice (E; 6–7 mice/group). Plots show mean with SEM and statistical evaluation (Student's t test).

See also Figure S5.

(4) c-Maf-induced genes (Ciofani et al., 2012), and (5) Th2 genes (Ranzani et al., 2015) (Figure 4E; Table S1). While the Th2 signature was not enriched in miR-221/222-deficient T lymphocytes, Th17 signatures were significantly enriched compared to WT CD4$^+$ T lymphocytes (Figures 4E and 4F). Notably, the IL-10 negative Th17 signature was more prominent than IL-10 positive Th17 signature, indicating a more proinflammatory nature of miR-221/222-deficient cells. In addition, the c-Maf-induced gene signature was enriched in miR-221/222-KO cells (Figure 4E), suggesting that c-Maf may be a key target downregulated by miR-221 and miR-222.

miR-221 and miR-222 target 3′UTR of *Maf* and *Il23r* for degradation to constrain Th17 response to IL-23

To examine the basis of the proclivity of miR-221/222-deficient Th17 cells to generate a proinflammatory signature, potential targets for miR-221 and miR-222 that are relevant to Th17 function were explored. A total of 2,827 putative targets were identified from an *in silico* prediction algorithm (microRNA.org; Betel et al., 2008), which were then cross-referenced to a list of core Th17 cell signature genes (Ciofani et al., 2012). Among the nine putative targets identified (Figure 5A), *Maf* and *Il23r* had potential target sequences in their 3′ untranslated region (3′ UTR) for miR-221 and miR-222 (Figures S5A and S5B) (Betel et al., 2008). *Maf* was of interest due to its essential role in regulating Th17 function and enrichment of its target genes in miR-221/222 KO cells (Figure 4E). *Il23r* drew our attention for its proinflammatory nature in Th17 cells and its upregulated expression in miR-221/222 KO cells (Figure S4) (Ciofani et al., 2012; Cua et al., 2003; Ghoreschi et al., 2010; Pfeifle et al., 2017; Tanaka et al., 2014) To validate *Maf* and *Il23r* as direct targets of miR-221 and miR-222, reporter constructs were generated with the 3′ UTR of *Maf* or *Il23r* fused to luciferase. Overexpression of miR-221 and miR-222 reduced luciferase activity compared to control miRNA (Figure 5B), indicating that both the 3′ UTR of *Maf* and *Il23r* mediated miR-221/222-dependent mRNA degradation of heterologous reporters.

Next, flow cytometry was used to test whether deletion of miR-221 and miR-222 resulted in elevated c-Maf protein expression in intestinal Th cells from WT and miR-221/222-KO mice. Consistent with previous studies, c-Maf was expressed higher in Treg and Th17 lymphocytes compared to naive CD4$^+$ T cells and Th1 cells from both WT and miR-221/222-KO mice (Figure 5C). Deletion of miR-221 and miR-222 resulted in increased c-Maf protein expression only in Th17 cells (Figure 5C). Of note, the expression of *Maf* and *Il23r* transcripts were largely comparable between WT and KO Th17 cells in steady-state condition, confirming the expected action of miRs at post-transcriptional and translational levels (Figure S5C). Next, to determine whether proinflammatory cytokine conditions further promote c-Maf expression in miR-221/222-deficient Th17 cells, small intestine lamina propria lymphocytes were stimulated *ex vivo* with IL-23 or IL-23 plus IL-1β. While these cytokines did not induce a change in c-Maf expression in Th17 cells from WT mice, c-Maf protein was significantly induced in Th17 from miR-221/222-KO mice (Figure 5D). In the same experiment, stimulation also

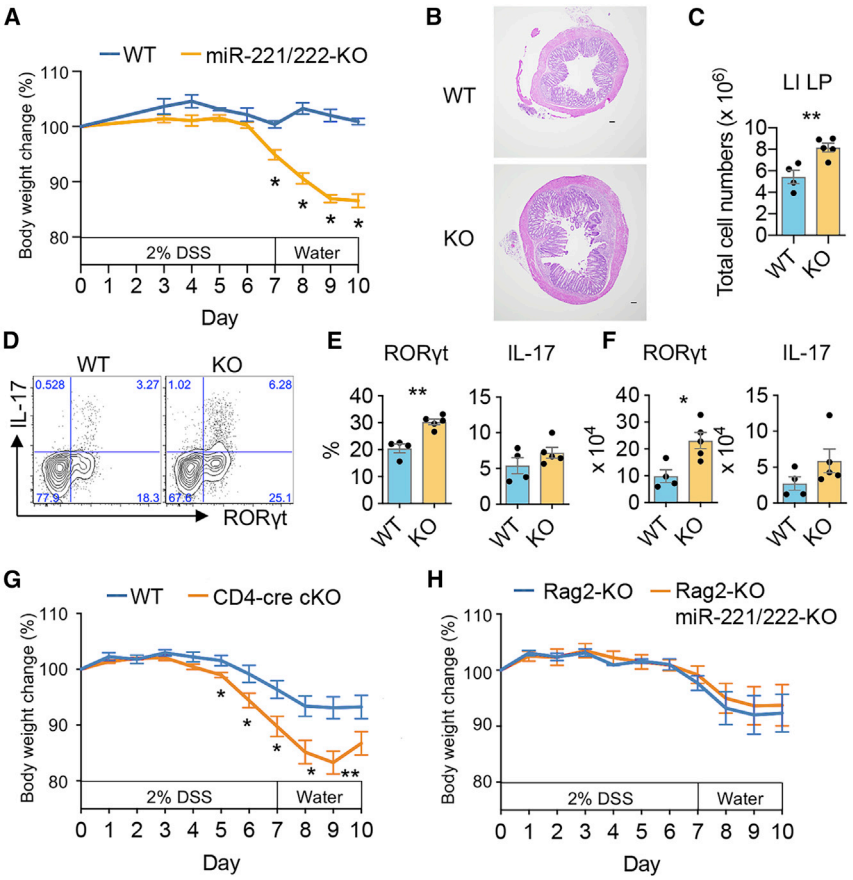

Figure 6. miR-221/222-KO and CD4-cre miR-221/222-conditional KO mice exhibit increased susceptibility to DSS-induced colitis

(A–F) WT (n = 4) and miR-221/222-KO (n = 5) mice were challenged with 2% DSS in drinking water to provoke intestinal inflammation. Data are representative of at least three independent experiments.

(A) Body weight change is expressed as a percentage of initial weight in WT and miR-221/222-KO mice. Statistically significant differences between WT and miR-221/222-KO mice are designated by asterisks (*p < 0.05).

(B) Representative H&E staining of colon specimens at day 10. A scale bar at the bottom right corner of each image represents 100 μm.

(C) Absolute cell numbers of colonic LPLs isolated from WT and miR-221/222-KO mice (**p < 0.01).

(D–F) Frequency (D and E) and absolute number (F) of RORγt$^+$ and IL-17$^+$ CD4$^+$ lamina propria cells from colons of WT and miR-221/222-KO mice. Colonic lamina propria cells were stimulated with PMA-I for 4 h before staining. Data are represented as mean with SEM. Replicates were compared for significance, *p < 0.05, **p < 0.01, Student's t test.

(G) WT (n = 6) and CD4-cre miR-221/222-conditional KO (n = 8) mice were challenged with 2% DSS in drinking water to provoke intestinal inflammation. Data provided represent mean ± SEM of the % body weight of pooled data from two independent experiments (*p < 0.05, **p < 0.01).

(H) Data provided represent mean ± SEM of the % body weight of *Rag2*-KO (n = 5) and *Rag2-Mir221-Mir222* double KO (n = 6) mice pooled from two independent experiments.

See also Figure S6.

led to an increase in the frequency of IL-17-producing Th17 cells from miR-221/222-KO mice compared to WT mice (Figure 5E). Collectively, these results suggest that miR-221 and miR-222 function as negative feedback regulators in a proinflammatory Th17 signaling circuit by directly downregulating a signal entry step (IL-23R) as well as reducing a downstream transcription factor (c-Maf).

Deficiency of miR-221 and miR-222 increases the susceptibility of DSS-induced colitis in mice

In the gut, Th17 cells can be protective and promote homeostasis or mediate pathology depending upon the circumstance. The pathogenic role of IL-23R on T lymphocytes is well established, and *IL23R* has been identified as an important susceptibility gene in inflammatory bowel diseases (Duerr et al., 2006). In healthy miR-221/222-deficient mice, we found no broad disruption of T cell homeostasis in the gut (Figures 3A–3C and 3F–3I). Nonetheless, over time, miR-221/222-deficient Th17 lymphocytes may still contribute to spontaneous intestinal inflammation due to their enhanced response to IL-23 in mice. Accordingly, when small intestine histology was evaluated in WT and miR-221/222-KO mice living in a standard pathogen-free facility (Figure S6A), the average pathology score was higher in miR-221/222-KO mice compared to WT mice. However, the differences did not reach a statistical significance. In contrast, we consistently found that miR-221/222-deficient T cells had exaggerated Th17 responses once activated by T cell receptor (TCR) mimic, inflammatory cytokines, or lymphopenic expansion environment (Figures 2E–2F, 3D, 3E, 4, and 5E). Thus, we hypothesized that miR-221 and miR-222, while not being critical in the steady state, may be more important for constraining inflammation during pathological perturbation. Using the DSS colitis model, miR-221/222-KO mice showed a significant reduction in body weight and a greater severity of colitis compared to the WT mice (Figures 6A and 6B). Correspondingly, deficiency of miR-221 and miR-222 also resulted in a significant increase in the total number of lamina propria-infiltrating cells and number of Th17 lymphocytes compared to WT mice (Figures 6C–6F), demonstrating that miR-221/222 KO are more susceptible to DSS-induced colitis.

To assess whether the abnormalities seen in the DSS model with global miR-221/222-KO mice could be attributed mainly to T cell fractions or other fractions (innate cells and epithelial lining cells), we generated two more genetic models of miR-221/222 deletion in T cells (*CD4-cre Mir221Mir222* conditional KO [cKO]) and non-T cell fractions (*Rag2-Mir221Mir222* dual KO [DKO]). While no major defect was noted in major lymphocyte populations in cKO mice (Figure S6B), cKO mice were also more susceptible to DSS colitis compared to WT mice (Figure 6G). By contrast, DKO mice did not exhibit enhanced weight loss compared to *Rag2*-KO control (Figure 6H), indicating that deletion of miR-221 and miR-222 in innate cell compartments

or epithelial cells did not compromise mice to DSS challenge to the same degree as deletion in T cells. Collectively, our findings indicate that miR-221 and miR-222 regulate response to DSS-mediated barrier damage mostly, if not exclusively, in a T cell intrinsic manner via modulating the magnitude of proinflammatory Th17 response induced by injury.

DISCUSSION

A growing body of evidence supports important regulatory roles of miRNAs in a wide range of biological and pathological processes by modulating multiple target mRNAs at a post-transcriptional stage (Bartel, 2018). miR-221 and miR-222, which reside in close proximity on chromosome X, have previously been dubbed as ''onco-miRNAs'' reflecting their expression in malignant cells and potential roles in cell proliferation, initiation, and progression of cancer (Garofalo et al., 2012). miR-221 and miR-222 were reported to play an important regulatory role in macrophage tolerance to LPS, and its high expression is relevant to predict immunoparalysis and poor prognosis of sepsis patients (Seeley et al., 2018). In this study, we reveal a previously unappreciated role of miR-221 and miR-222 in controlling Th17 cell response in the intestinal mucosa under proinflammatory conditions. miR-221 and miR-222 are critical negative feedback components that constrain IL-23-induced Th17 response by downregulating IL-23R and c-Maf. Accordingly, loss of miR-221 and miR-222 compromised the ability of miR-221/222-deffi-cient mice to protect against mucosal barrier damage.

To date, several miRNAs have been reported to contribute to Th17 cell differentiation (Baumjohann and Ansel, 2013). Loss of mature miRNAs in Dicer-deficient $CD4^+$ T cells shows reduced IL-17 production under Th17(β) condition (Cobb et al., 2006). Similarly, knocking out or knocking down miR-155, miR-326, miR-301a, miR-183c, miR-132, and miR-212 results in marked reduction of Th17 cells *in vitro* and *in vivo* (Du et al., 2009; Escobar et al., 2014; Ichiyama et al., 2016; Mycko et al., 2012; O'Connell et al., 2010). In contrast, some miRNAs have been shown to repress the development of Th17 cells, including miR-15b, miR-17~92 and miR-18a that target *Ogt*, *Rora*, and *Smad4* respectively (Liu et al., 2017). Our data add miR-221 and miR-222 to the list of Th17-regulating miRNAs with a very specialized window of action. miR-221 and miR-222 operate in a proinflammatory signal selective (IL-23) condition, but their action is muted in TGF-β dominant condition. This unique feature of miR-221 and miR-222 has an illuminating implication in understanding the regulatory mechanisms balancing divergent proinflammatory versus regulatory actions of Th17 cells.

Early on, phenotypic description of Th17 subpopulations was defined *in vitro* by different cytokines (Bettelli et al., 2006; Ghoreschi et al., 2010). TGF-β is thought to represent a regulatory feature of Th17 cells, whereas IL-23 represents a proinflammatory feature (Ghoreschi et al., 2010). From human Th17 clones, IL-10 was identified as a key marker representing an immunoregulatory and tissue resident program, whereas IL-10-negative Th17 cells were proinflammatory (Aschenbrenner et al., 2018). *In vivo* Th17 studies provided further insight into protective versus inflammatory features of tissue-resident Th17 cells, which underpinned differences in the microbiome. Homeostatic Th17 cells induced by commensal bacteria maintained muted memory-cell-like metabolism and did not participate in inflammatory reaction, whereas pathogen-induced Th17 cells were glycolytic, inflammatory, and produced IFN-γ (Omenetti et al., 2019). In this study, the observation that deficiency of miR-221 and miR-222 is tolerated and Th17 homeostasis is maintained in healthy hosts suggests that commensal-induced non-pathological Th17 cells are similar to TGF-β-induced regulatory Th17 cells; expression of miR-221 and miR-222 is muted under homeostatic conditions and functionally less critical. In contrast, miR-221 and miR-222 are more relevant during proinflammatory conditions, as they are upregulated by IL-23 and target *Il23r* for downregulation to constrain an otherwise feedforward circuit of proinflammatory Th17 response.

Another key target of miR-221 and miR-222 is *Maf* (protein c-Maf). Th17 cells express this transcription factor highly, and it is critical for several important aspects of Th17 differentiation and function (reviewed in Imbratta et al., 2020). In miR-221/222-KO mice, c-Maf expression was enhanced in Th17 cells and not naive, Th1, or Treg fractions isolated from the gut. In addition, *ex vivo* stimulation of miR-221/222-deficient gut lymphocytes with IL-23 resulted in more c-Maf and more IL-17-producing Th17 cells. c-Maf is a major regulator of cytokine loci, especially *Il17a* in Th17 cells and γδT cells (Ciofani et al., 2012; Tanaka et al., 2014; Zuberbuehler et al., 2019), suggesting that elevated c-Maf results in more IL-17 production in miR-221/222-deficient Th17 cells. Elevated c-Maf may also induce more IL-23R expression in miR-221/222-deficient Th17 cells, perpetuating a proinflammatory positive feedback loop. The *Il23r* gene contains a MARE-like sequence (Sato et al., 2011), but whether c-Maf induces or represses IL-23R expression remains unclear. Immunoregulatory or proinflammatory conditions may explain this discrepancy, as c-Maf represses *Il23r* expression in IL-10-positive Th17 cells (Aschenbrenner et al., 2018) and induces *Il23r* under IL-23 culture conditions (Bauquet et al., 2009). Considering the latter, our data suggest that c-Maf induces IL-23R in miR-221/222-deficient Th17 cells stimulated with IL-23, and normally miR-221 and miR-222 function to prevent this feedforward loop. As c-Maf shows broad, robust expression across an array of Th17 cells and has its own network of target genes, miR-221- and miR-222-mediated regulation may act via c-Maf independent of IL-23 signaling (Ciofani et al., 2012; Imbratta et al., 2020). Nonetheless, our data demonstrate that a relevant action of miR-221 and miR-222 is in the proinflammatory arm of Th17 response, and they act as inflammation-induced negative feedback regulators directly downregulating a signal entry step (IL-23R), as well as constraining a downstream transcription factor (c-Maf).

In a broader context, the current study, which places miR-221 and miR-222 as negative regulators of intestinal inflammatory Th17 response, aligns well with reported action of these miRs in innate cells. In macrophages, miR-221 and miR-222 induce transcriptional silencing of inflammatory genes downstream of LPS signaling, albeit through a different target molecule (*Brg1*) (Seeley et al., 2018). In this prior report, evaluation of sepsis patients revealed an association between higher expression of these miRs and poor clinical outcome (Seeley et al., 2018). Altogether, miR-221 and miR-222 may serve as a generalizable biomarker of immune response to proinflammatory environment adapted by both innate and adaptive cells. Further study is

warranted to pursue action of these miRs in broad array of immune cells as well as their potential as a biomarker of inflammation in various type of clinical settings.

Limitations of the study

This study is limited by its focus on evaluating the action of miR-221 and miR-222 in selected loss-of-function experimental settings and concentrating on cells isolated from the gut in mice. As inflammatory Th17 responses play a role beyond intestine, investigation into other forms of pathological inflammation in the skin or brain will be important to understand the broader impact of miR-221 and miR-222. Moreover, miRNAs typically target numerous gene transcripts, so our analysis undoubtedly misses many other relevant targets in a wide variety of cells in diverse environments. Furthermore, the relevance of miR-221 and miR-222 in human inflammatory bowel diseases has not been addressed in this study.

STAR★METHODS

Detailed methods are provided in the online version of this paper and include the following:

- KEY RESOURCES TABLE
- RESOURCE AVAILABILITY
  - Lead contact
  - Material availability
  - Data and code availability
- EXPERIMENTAL MODEL AND SUBJECT DETAILS
- METHOD DETAILS
  - Mice
  - Preparation of cell suspensions from tissues
  - Cell culture
  - Flow cytometry
  - Library preparation for RNA Sequencing (small RNA-seq and mRNA-seq)
  - Library preparation for Single cell RNA-sequencing (scRNA-seq)
  - Chromatin immunoprecipitation sequencing (ChIP-seq)
  - RT-qPCR
  - Luciferase assay
  - DSS-induced colitis
  - Histology
  - Microbiome analysis
- QUANTIFICATION AND STATISTICAL ANALYSIS
  - mRNA-seq analysis
  - microRNA-seq analysis
  - scRNA-seq analysis

SUPPLEMENTAL INFORMATION

Supplemental Information can be found online at https://doi.org/10.1016/j.immuni.2021.02.015.

ACKNOWLEDGMENTS

We thank J. Simone, J. Lay, K. Tinsley (NIAMS) for flow cytometry; G. Gutierrez-Cruz, S. Dell'Orso, F. Naz (NIAMS) for deep sequencing; K. Jiang and Dimitrios Anastasakis (NIAMS) for bioinformatics support; Ivan Fuss (NIAID) for histopathologic scoring; and the NIAMS LACU staff and Y. Morimoto (NIAMS) for their technical support to handle mice. We thank Vanja Lazarevic (NCI) and Mark Ansel (UCSF) for critical reading, the members of the O'Shea laboratory for helpful discussions, and Tomoya Kanno for graphics. This study utilized the high-performance computational capabilities of the Biowulf Linux cluster at the NIH. This work was supported by the Intramural Research Programs of NIAMS and NIAID. Y.M. was supported by Japan Society for the Promotion of Science (JSPS) KAKENHI Grant-in-Aid (B) 20H03666 and Japanese Researcher Fellowships at NIH. R.L.P. was supported by a Postdoctoral Research Associate (PRAT) fellowship from the National Institute of General Medical Sciences (NIGMS), award number 1Fi2GM137942-01.

AUTHOR CONTRIBUTIONS

Conceptualization, Y.M. and J.J.O.; methodology, Y.M. and H.T.; software, Y.M., F.P.D., H.-W.S., and S.R.B.; validation, Y.M., R.L.P., and S.R.B.; formal analysis, Y.M., R.L.P., S.R.B., and F.P.D.; investigation, Y.M., R.L.P., G.S., F.P., H.N., C.Y., F.M., A.C.P., H.-Y.S., B.A., and Y.K.; writing, Y.M., R.L.P., Y.K., and J.J.O.; visualization, Y.M., R.L.P., and S.R.B.; supervision, S.A.M., M.H., Y.K., and J.J.O.; funding acquisition, M.H., S.A.M., and J.J.O.

DECLARATION OF INTERESTS

The authors declare no competing financial interests. J.J.O. is a member of the advisory board of *Immunity*.

Received: July 15, 2020
Revised: December 8, 2020
Accepted: February 12, 2021
Published: March 2, 2021

REFERENCES

Aschenbrenner, D., Foglierini, M., Jarrossay, D., Hu, D., Weiner, H.L., Kuchroo, V.K., Lanzavecchia, A., Notarbartolo, S., and Sallusto, F. (2018). An immunoregulatory and tissue-residency program modulated by c-MAF in human T_H17 cells. Nat. Immunol. *19*, 1126–1136.

Bartel, D.P. (2018). Metazoan MicroRNAs. Cell *173*, 20–51.

Baumjohann, D., and Ansel, K.M. (2013). MicroRNA-mediated regulation of T helper cell differentiation and plasticity. Nat. Rev. Immunol. *13*, 666–678.

Bauquet, A.T., Jin, H., Paterson, A.M., Mitsdoerffer, M., Ho, I.-C., Sharpe, A.H., and Kuchroo, V.K. (2009). The costimulatory molecule ICOS regulates the expression of c-Maf and IL-21 in the development of follicular T helper cells and TH-17 cells. Nat. Immunol. *10*, 167–175.

Betel, D., Wilson, M., Gabow, A., Marks, D.S., and Sander, C. (2008). The microRNA.org resource: targets and expression. Nucleic Acids Res *36*, D149–D153.

Bettelli, E., Carrier, Y., Gao, W., Korn, T., Strom, T.B., Oukka, M., Weiner, H.L., and Kuchroo, V.K. (2006). Reciprocal developmental pathways for the generation of pathogenic effector TH17 and regulatory T cells. Nature *441*, 235–238.

Ciofani, M., Madar, A., Galan, C., Sellars, M., Mace, K., Pauli, F., Agarwal, A., Huang, W., Parkhurst, C.N., Muratet, M., et al. (2012). A validated regulatory network for Th17 cell specification. Cell *151*, 289–303.

Cobb, B.S., Hertweck, A., Smith, J., O'Connor, E., Graf, D., Cook, T., Smale, S.T., Sakaguchi, S., Livesey, F.J., Fisher, A.G., and Merkenschlager, M. (2006). A role for Dicer in immune regulation. J. Exp. Med. *203*, 2519–2527.

Cua, D.J., Sherlock, J., Chen, Y., Murphy, C.A., Joyce, B., Seymour, B., Lucian, L., To, W., Kwan, S., Churakova, T., et al. (2003). Interleukin-23 rather than interleukin-12 is the critical cytokine for autoimmune inflammation of the brain. Nature *421*, 744–748.

Du, C., Liu, C., Kang, J., Zhao, G., Ye, Z., Huang, S., Li, Z., Wu, Z., and Pei, G. (2009). MicroRNA miR-326 regulates TH-17 differentiation and is associated with the pathogenesis of multiple sclerosis. Nat. Immunol. *10*, 1252–1259.

Duerr, R.H., Taylor, K.D., Brant, S.R., Rioux, J.D., Silverberg, M.S., Daly, M.J., Steinhart, A.H., Abraham, C., Regueiro, M., Griffiths, A., et al. (2006). A

genome-wide association study identifies IL23R as an inflammatory bowel disease gene. Science *314*, 1461–1463.

Escobar, T.M., Kanellopoulou, C., Kugler, D.G., Kilaru, G., Nguyen, C.K., Nagarajan, V., Bhairavabhotla, R.K., Northrup, D., Zahr, R., Burr, P., et al. (2014). miR-155 activates cytokine gene expression in Th17 cells by regulating the DNA-binding protein Jarid2 to relieve polycomb-mediated repression. Immunity *40*, 865–879.

Esplugues, E., Huber, S., Gagliani, N., Hauser, A.E., Town, T., Wan, Y.Y., O'Connor, W., Jr., Rongvaux, A., Van Rooijen, N., Haberman, A.M., et al. (2011). Control of TH17 cells occurs in the small intestine. Nature *475*, 514–518.

Gaffen, S.L., Jain, R., Garg, A.V., and Cua, D.J. (2014). The IL-23-IL-17 immune axis: from mechanisms to therapeutic testing. Nat. Rev. Immunol. *14*, 585–600.

Garofalo, M., Quintavalle, C., Romano, G., Croce, C.M., and Condorelli, G. (2012). miR221/222 in cancer: their role in tumor progression and response to therapy. Curr. Mol. Med. *12*, 27–33.

Gaublomme, J.T., Yosef, N., Lee, Y., Gertner, R.S., Yang, L.V., Wu, C., Pandolfi, P.P., Mak, T., Satija, R., Shalek, A.K., et al. (2015). Single-Cell Genomics Unveils Critical Regulators of Th17 Cell Pathogenicity. Cell *163*, 1400–1412.

Ghoreschi, K., Laurence, A., Yang, X.-P., Tato, C.M., McGeachy, M.J., Konkel, J.E., Ramos, H.L., Wei, L., Davidson, T.S., Bouladoux, N., et al. (2010). Generation of pathogenic T(H)17 cells in the absence of TGF-β signalling. Nature *467*, 967–971.

Hirahara, K., Onodera, A., Villarino, A.V., Bonelli, M., Sciumè, G., Laurence, A., Sun, H.-W., Brooks, S.R., Vahedi, G., Shih, H.-Y., et al. (2015). Asymmetric Action of STAT Transcription Factors Drives Transcriptional Outputs and Cytokine Specificity. Immunity *42*, 877–889.

Hnisz, D., Abraham, B.J., Lee, T.I., Lau, A., Saint-André, V., Sigova, A.A., Hoke, H.A., and Young, R.A. (2013). Super-enhancers in the control of cell identity and disease. Cell *155*, 934–947.

Ichiyama, K., Gonzalez-Martin, A., Kim, B.-S., Jin, H.Y., Jin, W., Xu, W., Sabouri-Ghomi, M., Xu, S., Zheng, P., Xiao, C., and Dong, C. (2016). The MicroRNA-183-96-182 Cluster Promotes T Helper 17 Cell Pathogenicity by Negatively Regulating Transcription Factor Foxo1 Expression. Immunity *44*, 1284–1298.

Imbratta, C., Hussein, H., Andris, F., and Verdeil, G. (2020). c-MAF, a Swiss Army Knife for Tolerance in Lymphocytes. Front. Immunol. *11*, 206.

Ivanov, I.I., McKenzie, B.S., Zhou, L., Tadokoro, C.E., Lepelley, A., Lafaille, J.J., Cua, D.J., and Littman, D.R. (2006). The orphan nuclear receptor RORgammat directs the differentiation program of proinflammatory IL-17+ T helper cells. Cell *126*, 1121–1133.

Ivanov, I.I., Atarashi, K., Manel, N., Brodie, E.L., Shima, T., Karaoz, U., Wei, D., Goldfarb, K.C., Santee, C.A., Lynch, S.V., et al. (2009). Induction of intestinal Th17 cells by segmented filamentous bacteria. Cell *139*, 485–498.

Kaplan, M.H., Sun, Y.L., Hoey, T., and Grusby, M.J. (1996). Impaired IL-12 responses and enhanced development of Th2 cells in Stat4-deficient mice. Nature *382*, 174–177.

Kent, W.J., Zweig, A.S., Barber, G., Hinrichs, A.S., and Karolchik, D. (2010). BigWig and BigBed: enabling browsing of large distributed datasets. Bioinformatics *26*, 2204–2207.

Korn, T., Bettelli, E., Oukka, M., and Kuchroo, V.K. (2009). IL-17 and Th17 Cells. Annu. Rev. Immunol. *27*, 485–517.

Kozich, J.J., Westcott, S.L., Baxter, N.T., Highlander, S.K., and Schloss, P.D. (2013). Development of a dual-index sequencing strategy and curation pipeline for analyzing amplicon sequence data on the MiSeq Illumina sequencing platform. Appl. Environ. Microbiol. *79*, 5112–5120.

Kuchen, S., Resch, W., Yamane, A., Kuo, N., Li, Z., Chakraborty, T., Wei, L., Laurence, A., Yasuda, T., Peng, S., et al. (2010). Regulation of microRNA expression and abundance during lymphopoiesis. Immunity *32*, 828–839.

Langmead, B., Trapnell, C., Pop, M., and Salzberg, S.L. (2009). Ultrafast and memory-efficient alignment of short DNA sequences to the human genome. Genome Biol. *10*, R25.

Langrish, C.L., Chen, Y., Blumenschein, W.M., Mattson, J., Basham, B., Sedgwick, J.D., McClanahan, T., Kastelein, R.A., and Cua, D.J. (2005). IL-23 drives a pathogenic T cell population that induces autoimmune inflammation. J. Exp. Med. *201*, 233–240.

Lee, Y., Awasthi, A., Yosef, N., Quintana, F.J., Xiao, S., Peters, A., Wu, C., Kleinewietfeld, M., Kunder, S., Hafler, D.A., et al. (2012). Induction and molecular signature of pathogenic TH17 cells. Nat. Immunol. *13*, 991–999.

Lee, C.-K., Raz, R., Gimeno, R., Gertner, R., Wistinghausen, B., Takeshita, K., DePinho, R.A., and Levy, D.E. (2002). STAT3 is a negative regulator of granulopoiesis but is not required for G-CSF-dependent differentiation. Immunity *17*, 63–72.

Littman, D.R., and Rudensky, A.Y. (2010). Th17 and regulatory T cells in mediating and restraining inflammation. Cell *140*, 845–858.

Liu, R., Ma, X., Chen, L., Yang, Y., Zeng, Y., Gao, J., Jiang, W., Zhang, F., Li, D., Han, B., et al. (2017). MicroRNA-15b Suppresses Th17 Differentiation and Is Associated with Pathogenesis of Multiple Sclerosis by Targeting *O*-GlcNAc Transferase. J. Immunol. *198*, 2626–2639.

Mycko, M.P., Cichalewska, M., Machlanska, A., Cwiklinska, H., Mariasiewicz, M., and Selmaj, K.W. (2012). MicroRNA-301a regulation of a T-helper 17 immune response controls autoimmune demyelination. Proc. Natl. Acad. Sci. USA *109*, E1248–E1257.

O'Connell, R.M., Kahn, D., Gibson, W.S.J., Round, J.L., Scholz, R.L., Chaudhuri, A.A., Kahn, M.E., Rao, D.S., and Baltimore, D. (2010). MicroRNA-155 promotes autoimmune inflammation by enhancing inflammatory T cell development. Immunity *33*, 607–619.

O'Shea, J.J., and Paul, W.E. (2010). Mechanisms underlying lineage commitment and plasticity of helper CD4+ T cells. Science *327*, 1098–1102.

Omenetti, S., Bussi, C., Metidji, A., Iseppon, A., Lee, S., Tolaini, M., Li, Y., Kelly, G., Chakravarty, P., Shoaie, S., et al. (2019). The Intestine Harbors Functionally Distinct Homeostatic Tissue-Resident and Inflammatory Th17 Cells. Immunity *51*, 77–89.e6.

Patel, D.D., and Kuchroo, V.K. (2015). Th17 Cell Pathway in Human Immunity: Lessons from Genetics and Therapeutic Interventions. Immunity *43*, 1040–1051.

Pfeifle, R., Rothe, T., Ipseiz, N., Scherer, H.U., Culemann, S., Harre, U., Ackermann, J.A., Seefried, M., Kleyer, A., Uderhardt, S., et al. (2017). Regulation of autoantibody activity by the IL-23-T_H17 axis determines the onset of autoimmune disease. Nat. Immunol. *18*, 104–113.

Pruitt, K.D., Harrow, J., Harte, R.A., Wallin, C., Diekhans, M., Maglott, D.R., Searle, S., Farrell, C.M., Loveland, J.E., Ruef, B.J., et al. (2009). The consensus coding sequence (CCDS) project: Identifying a common protein-coding gene set for the human and mouse genomes. Genome Res. *19*, 1316–1323.

Quast, C., Pruesse, E., Yilmaz, P., Gerken, J., Schweer, T., Yarza, P., Peplies, J., and Glöckner, F.O. (2013). The SILVA ribosomal RNA gene database project: improved data processing and web-based tools. Nucleic Acids Res. *41*, D590–D596.

Quinlan, A.R., and Hall, I.M. (2010). BEDTools: a flexible suite of utilities for comparing genomic features. Bioinformatics *26*, 841–842.

Quintana, F.J., Basso, A.S., Iglesias, A.H., Korn, T., Farez, M.F., Bettelli, E., Caccamo, M., Oukka, M., and Weiner, H.L. (2008). Control of T(reg) and T(H)17 cell differentiation by the aryl hydrocarbon receptor. Nature *453*, 65–71.

Ranzani, V., Rossetti, G., Panzeri, I., Arrigoni, A., Bonnal, R.J., Curti, S., Gruarin, P., Provasi, E., Sugliano, E., Marconi, M., et al. (2015). The long intergenic noncoding RNA landscape of human lymphocytes highlights the regulation of T cell differentiation by linc-MAF-4. Nat. Immunol. *16*, 318–325.

Rutz, S., Noubade, R., Eidenschenk, C., Ota, N., Zeng, W., Zheng, Y., Hackney, J., Ding, J., Singh, H., and Ouyang, W. (2011). Transcription factor c-Maf mediates the TGF-β-dependent suppression of IL-22 production in T(H)17 cells. Nat. Immunol. *12*, 1238–1245.

Satija, R., Farrell, J.A., Gennert, D., Schier, A.F., and Regev, A. (2015). Spatial reconstruction of single-cell gene expression data. Nat. Biotechnol. *33*, 495–502.

Sato, K., Miyoshi, F., Yokota, K., Araki, Y., Asanuma, Y., Akiyama, Y., Yoh, K., Takahashi, S., Aburatani, H., and Mimura, T. (2011). Marked induction of c-Maf

protein during Th17 cell differentiation and its implication in memory Th cell development. J. Biol. Chem. *286*, 14963–14971.

Schraml, B.U., Hildner, K., Ise, W., Lee, W.-L., Smith, W.A.-E., Solomon, B., Sahota, G., Sim, J., Mukasa, R., Cemerski, S., et al. (2009). The AP-1 transcription factor Batf controls T(H)17 differentiation. Nature *460*, 405–409.

Sciumé, G., Hirahara, K., Takahashi, H., Laurence, A., Villarino, A.V., Singleton, K.L., Spencer, S.P., Wilhelm, C., Poholek, A.C., Vahedi, G., et al. (2012). Distinct requirements for T-bet in gut innate lymphoid cells. J. Exp. Med. *209*, 2331–2338.

Seeley, J.J., Baker, R.G., Mohamed, G., Bruns, T., Hayden, M.S., Deshmukh, S.D., Freedberg, D.E., and Ghosh, S. (2018). Induction of innate immune memory via microRNA targeting of chromatin remodelling factors. Nature *559*, 114–119.

Segata, N., Izard, J., Waldron, L., Gevers, D., Miropolsky, L., Garrett, W.S., and Huttenhower, C. (2011). Metagenomic biomarker discovery and explanation. Genome Biol. *12*, R60.

Shih, H.-Y., Sciumè, G., Mikami, Y., Guo, L., Sun, H.-W., Brooks, S.R., Urban, J.F., Jr., Davis, F.P., Kanno, Y., and O'Shea, J.J. (2016). Developmental Acquisition of Regulomes Underlies Innate Lymphoid Cell Functionality. Cell *165*, 1120–1133.

Stockinger, B., and Omenetti, S. (2017). The dichotomous nature of T helper 17 cells. Nat. Rev. Immunol. *17*, 535–544.

Takahashi, H., Kanno, T., Nakayamada, S., Hirahara, K., Sciumè, G., Muljo, S.A., Kuchen, S., Casellas, R., Wei, L., Kanno, Y., and O'Shea, J.J. (2012). TGF-β and retinoic acid induce the microRNA miR-10a, which targets Bcl-6 and constrains the plasticity of helper T cells. Nat. Immunol. *13*, 587–595.

Tanaka, S., Suto, A., Iwamoto, T., Kashiwakuma, D., Kagami, S., Suzuki, K., Takatori, H., Tamachi, T., Hirose, K., Onodera, A., et al. (2014). Sox5 and c-Maf cooperatively induce Th17 cell differentiation via RORγt induction as downstream targets of Stat3. J. Exp. Med. *211*, 1857–1874.

Thorvaldsdóttir, H., Robinson, J.T., and Mesirov, J.P. (2013). Integrative Genomics Viewer (IGV): high-performance genomics data visualization and exploration. Brief. Bioinform. *14*, 178–192.

Trapnell, C., Roberts, A., Goff, L., Pertea, G., Kim, D., Kelley, D.R., Pimentel, H., Salzberg, S.L., Rinn, J.L., and Pachter, L. (2012). Differential gene and transcript expression analysis of RNA-seq experiments with TopHat and Cufflinks. Nature Protocols *7*, 562–578.

Vahedi, G., Takahashi, H., Nakayamada, S., Sun, H.-W., Sartorelli, V., Kanno, Y., and O'Shea, J.J. (2012). STATs shape the active enhancer landscape of T cell populations. Cell *151*, 981–993.

Veldhoen, M., Hirota, K., Westendorf, A.M., Buer, J., Dumoutier, L., Renauld, J.-C., and Stockinger, B. (2008). The aryl hydrocarbon receptor links TH17-cell-mediated autoimmunity to environmental toxins. Nature *453*, 106–109.

Wei, L., Vahedi, G., Sun, H.-W., Watford, W.T., Takatori, H., Ramos, H.L., Takahashi, H., Liang, J., Gutierrez-Cruz, G., Zang, C., et al. (2010). Discrete roles of STAT4 and STAT6 transcription factors in tuning epigenetic modifications and transcription during T helper cell differentiation. Immunity *32*, 840–851.

Yang, X.O., Panopoulos, A.D., Nurieva, R., Chang, S.H., Wang, D., Watowich, S.S., and Dong, C. (2007). STAT3 regulates cytokine-mediated generation of inflammatory helper T cells. J. Biol. Chem. *282*, 9358–9363.

Yosef, N., Shalek, A.K., Gaublomme, J.T., Jin, H., Lee, Y., Awasthi, A., Wu, C., Karwacz, K., Xiao, S., Jorgolli, M., et al. (2013). Dynamic regulatory network controlling TH17 cell differentiation. Nature *496*, 461–468.

Zhang, Y., Liu, T., Meyer, C.A., Eeckhoute, J., Johnson, D.S., Bernstein, B.E., Nusbaum, C., Myers, R.M., Brown, M., Li, W., and Liu, X.S. (2008). Model-based analysis of ChIP-Seq (MACS). Genome Biol. *9*, R137.

Zhu, J., Yamane, H., and Paul, W.E. (2010). Differentiation of effector CD4 T cell populations (*). Annu. Rev. Immunol. *28*, 445–489.

Zuberbuehler, M.K., Parker, M.E., Wheaton, J.D., Espinosa, J.R., Salzler, H.R., Park, E., and Ciofani, M. (2019). The transcription factor c-Maf is essential for the commitment of IL-17-producing γδ T cells. Nat. Immunol. *20*, 73–85.

STAR★METHODS

KEY RESOURCES TABLE

REAGENT or RESOURCE	SOURCE	IDENTIFIER
Antibodies		
Anti-K4m1 antibody	Abcam	ab8895; RRID: AB_306847
Anti-K4m3 antibody	Abcam	ab8580; RRID:AB_306649
Anti-K27m3 antibody	Millipore	07-449; RRID:AB_310624
Anti-p300 antibody	Santa Cruz Biotechnology	sc-585; RRID:AB_2231120
Anti-STAT3 antibody	Thermo Fisher Scientific	14-6727-81; RRID:AB_468247
anti-CD3 antibody	Thermo Fisher Scientific	16-0031-86; RRID:AB_468849
anti-CD3 antibody	BioxCell	BE0001-1; RRID:AB_1107634
anti-CD28 antibody	Thermo Fisher Scientific	16-0281-86; RRID:AB_468923
anti-CD28 antibody	BioxCell	BE0015-1; RRID:AB_1107624
anti-IFN-γ antibody	BioXCell	BE0055; RRID:AB_1107694
anti-IL-4 antibody	BioXCell	BE0045; RRID:AB_1107707
anti-CD4 antibody	BD Biosciences	550954; RRID:AB_393977
anti-CD8 antibody	BD Biosciences	551162; RRID:AB_394081
anti-CD25 antibody	Thermo Fisher Scientific	17-0251-81; RRID:AB_469365
anti-CD44 antibody	Thermo Fisher Scientific	12-0441-81; RRID:AB_465663
anti-CD45.1 antibody	BD Biosciences	17-0453-81; RRID:AB_469397
anti-CD45.2 antibody	BioLegend	48-0454-80; RRID:AB_11039533
anti-CD62L antibody	Thermo Fisher Scientific	25-0621-81; RRID:AB_469632
anti-c-Kit antibody	BD Biosciences	553354; RRID:AB_394805
anti-Sca-1 antibody	BioLegend	108112; RRID:AB_313349
anti-Nkp46antibody	Thermo Fisher Scientific	46-3351-82; RRID:AB_1834441
anti-RORgt antibody	BD Biosciences	562607; RRID:AB_11153137
anti-T-bet antibody	Thermo Fisher Scientific	25-5825-82; RRID:AB_11042699
anti-Foxp3 antibody	Thermo Fisher Scientific	48-5773-82; RRID:AB_1518812
anti-IL-17A antibody	BioLegend	506922; RRID:AB_2125010
anti-IFN-γ antibody	Thermo Fisher Scientific	17-7311-81; RRID:AB_469503
anti-IL-4 antibody	BioLegend	504120; RRID:AB_2562102
anti-IL-13 antibody	Thermo Fisher Scientific	50-7133-82; RRID:AB_2574279
anti-TCR γ/δ antibody	BioLegend	118118; RRID:AB_10612756
anti-IL-2 antibody	BioxCell	BE0043-1; RRID:AB_1107705
anti-c-MAF Monoclonal Antibody (sym0F1), PE	Thermo Fisher Scientific	Cat # 12-9855-42; RRID:AB_2572747
Prime Flow c-Maf probe (Assay ID: VB6-14037-PF), Alexa Fluor 750	Thermo Fisher Scientific	Cat # PF-204
Prime Flow Il23r probe (Assay ID: VB1-17154-PF), Alexa Fluor 647	Thermo Fisher Scientific	Cat # PF-204
PrimeFlow™ RNA Assay Kit, 40 tests	Thermo Fisher Scientific	Cat # 88-18005-204
Chemicals, Peptides, and Recombinant Proteins		
Recombinant Human TGF-β1	R&D Systems	240-B-010
Recombinant Mouse IL-1 beta	R&D Systems	401-ML-005
Recombinant Mouse IL-12	R&D Systems	419-ML-010
Recombinant Mouse IL-23	R&D Systems	1887-ML-010
Recombinant Mouse IL-6	R&D Systems	406-ML-005

(*Continued on next page*)

Continued

REAGENT or RESOURCE	SOURCE	IDENTIFIER
Human IL-2	National Cancer Institute	N/A
Dextran sulfate sodium salt	MP Biomedicals	160110
Critical Commercial Assays		
TruSeq RNA Sample Prep Kit v2	Illumina	RS-122-2001
TruSeq Small RNA Sample Prep Kit	illumina	RS-200-0012
Luc-Pair Duo-Luciferase Assay Kits 2.0	GeneCopoeia	LF-001
Lipofectamine LTX with Plus Reagent	Thermo Fisher Scientific	A12621
TaqMan Reverse Transcription Kit	Thermo Fisher Scientific	4366597
TaqMan® Universal PCR Master Mix, No AmpErase® UNG	Thermo Fisher Scientific	4364341
TRIzol	Thermo Fisher Scientific	15596018
mirVana miRNA Isolation Kit	Thermo Fisher Scientific	AM1560
Chromium Single Cell 3′ Reagent kits v2	10x Genomics	PN-120237
Zombie NIR Fixable Viability kit	Biolegend	Cat #: 423105
Deposited Data		
Raw and analyzed data	This paper	GEO: GSE160250
ChIP-seq samples for p300 and K4me1 (Th1)	Vahedi et al., 2012	GEO: GSE40463
ChIP-seq samples for STAT4 (Th1)	Wei et al., 2010	GEO: GSE22104
ChIP-seq samples for STAT3 and K27me3 (Th17)	Ghoreschi et al., 2010	GEO: GSE23681
ChIP-seq samples for calling super enhancers (Th cells)	Hnisz et al., 2013	GEO: GSE17312
Consensus coding sequence	Pruitt et al., 2009	Genome Res. 2009 Jul; 19(7): 1316–1323.
Experimental Models: Cell Lines		
HEK293T	ATCC	CRL-3216
Experimental Models: Organisms/Strains		
C57BL/6J (WT)	The Jackson Laboratory	#000664
B6.SJL-Ptprc^{a}/BoyAiTac (CD45.1+)	Taconic	#4007
C57BL/6-Il17atm1Bcgen/J (Il17a-GFP)	The Jackson Laboratory	#018472
C.B6 (Cg)-Rag2tm1.1Cgn/J (Rag2−/−)	The Jackson Laboratory	#008448
B6.Cg-Tg(Cd4-cre)1Cwi/BfluJ	The Jackson Laboratory	# 017336
CD4-Cre-STAT3fl/fl	Dr. David E. Levy (NYU)	N/A
STAT4 KO	Dr. Mark Kaplan (IU)	N/A
C57BL/6-Mir221/222 fl/fl	This paper	N/A
Mir221/222 KO	This paper	N/A
CD4-Cre-mir221/222 fl/fl (conditional KO: cKO)	This paper	N/A
Rag2-miR-221/222 (double KO: DKO)	This paper	N/A
IL17-GFP miR-221/222 KO	This paper	N/A
Oligonucleotides		
TaqMan® miRNA Assay (snoRNA202)	Thermo Fisher Scientific	4427975-001232
TaqMan® miRNA Assay (hsa-miR-221)	Thermo Fisher Scientific	4427975-000524
TaqMan® miRNA Assay (hsa-miR-222)	Thermo Fisher Scientific	4427975-002276
miRIDIAN microRNA Mimic (mmu-miR-221-3p)	Dharmacon	C-310583-07-0005
miRIDIAN microRNA Mimic (mmu-miR-222-3p)	Dharmacon	C-310584-07-0005
miRIDIAN microRNA Mimic Negative Control	Dharmacon	CN-001000-01-05

(*Continued on next page*)

Continued

REAGENT or RESOURCE	SOURCE	IDENTIFIER
Recombinant DNA		
miRNA 3′ UTR target clones for Maf	GeneCopoeia	MmiT024436-MT06
miRNA 3′ UTR target clones for Il23r	GeneCopoeia	MmiT038074-MT06
miRNA Target clone control vector for pEZX-MT06	GeneCopoeia	CmiT000001-MT06
Software and Algorithms		
BEDTOOLS	Quinlan and Hall, 2010	https://bedtools.readthedocs.io/en/latest/index.html
bedGraphToBigWig	Kent et al., 2010	https://genome.ucsc.edu/goldenpath/help/bigWig.html
wigToBigWig	Kent et al., 2010	https://genome.ucsc.edu/goldenpath/help/bigWig.html
The Integrative Genomics Viewer (IGV)	Thorvaldsdóttir et al., 2013	http://software.broadinstitute.org/software/igv/
Bowtie v1.1.2	Langmead et al., 2009	http://bowtie-bio.sourceforge.net/index.shtml
Cufflinks v 2.2.1	Trapnell et al., 2012	https://github.com/cole-trapnell-lab/cufflinks
MACS v 1.4.3	Zhang et al., 2008	https://pypi.org/project/MACS/
Seurat R package 3.1.5	Satija et al., 2015	https://satijalab.org/seurat/
R studio	RStudio	https://www.rstudio.com/
Partek Genome Suite v6.6	Partek Incorporated.	https://www.partek.com/
Prism software	GraphPad	RRID: SCR_002798
FlowJo v 9, v 10	BD Biosciences	RRID: SCR_008520
Other		
NGS data generated in this study	GEO	GSE160250

RESOURCE AVAILABILITY

Lead contact

John O'Shea (john.oshea@nih.gov).

Material availability

Further information and requests for resources and reagents should be directed to and will be fulfilled by the Lead Contact, John O'Shea, at NIH.

Data and code availability

All sequencing data generated during this study are available at Gene Expression Omnibus under the accession number GSE160250. Other source data used in the paper are summarized in supplemental Table S1 and analysis pipelines used are listed in key resources table.

EXPERIMENTAL MODEL AND SUBJECT DETAILS

All animal experiments were performed in the AAALAC-accredited animal housing facilities at NIH. All animal studies were performed according to the NIH guidelines for the use and care of live animals and were approved by the Institutional Animal Care and Use Committee of NIAMS. Mice of 6 −12 weeks old were used in all experiments. For sample size, see corresponding figure legends.

METHOD DETAILS

Mice

C57BL/6J, B6.Cg-Tg(Cd4-cre)1Cwi/BfluJ, C.B6 (Cg)-*Rag2*$^{tm1.1Cgn}$/*J* (*Rag2*-KO), and C57BL/6-*Il17a*^{tm1Bcgen}/J (*Il17a*-GFP) were purchased from Jackson Laboratory. B6.SJL-Ptprc^{a}/BoyAiTac (CD45.1+) were purchased from Taconic. *Stat3*$^{fl/fl}$ mice were from Dr. David Levy (Lee et al., 2002) and bred with CD4-Cre Tg mice. *Stat4* KO mice were from Dr. Mark Kaplan (Indiana University). C57BL/6-*Mir221Mir222* $^{fl/fl}$ mice and miR-221/222-KO (*Mir221Mir222* KO) mice were generated as described in Figure 2A and

Figure S2A. C57BL/6-*Mir221Mir222* $^{fl/fl}$ mice were bred with CD4-Cre to generate miR-221/222 conditional KO (cKO). Germline *Mir221Mir222* KO mice were bred with *Rag2*-KO to generate *Rag2-miR-221/222* double KO mice. *Il17a*-GFP mice were bred with *Mir221Mir222* KO to generate IL17-GFP-miR-221/222-KO.

For some experiments, WT (*Mir221Mir222* $^{fl/fl}$) and miR-221/222 KO mice were cohoused for at least 12 weeks starting at 3-4 weeks old so that microbiota of the gut is shared among them. Cohoused mice were used for the following experiments (Figures 3A–3C and 5C–5E).

For generation of bone marrow chimera mice *Rag2*-KO recipient mice were conditioned with 450 Rads prior to injection of 3 million donor BM cells (CD45.1+ and miR-221/222-KO). Mice were then fed Trimethoprim/Sulfamethoxazole antibiotics via drinking water for 5 weeks.

Preparation of cell suspensions from tissues

All cells were cultured in RPMI medium with 10% (vol/vol) FCS, 2 mM glutamine, 100 IU/mL of penicillin, 0.1 mg/mL, of streptomycin and 20 mM HEPES buffer, pH 7.2-7.5, 1 mM sodium pyruvate, nonessential amino acids (all from Thermo Fisher Scientific), and 2 μM β–mercaptoethanol (Sigma-Aldrich).

Cells from bone marrow, liver, lymph node and spleen were obtained by mechanical disruption. Cells from intestinal lamina propria were isolated after incubating fine-cut intestine in HBSS solution with 0.5 mg/mL DNase I (10104159001, Sigma-Aldrich) and 0.25 mg/mL Liberase TL (05401020001, Sigma-Aldrich) followed by filtering with 100 μm cell strainer and purification with 40% Percoll (6505, GE) (Sciumé et al., 2012). Isolated cells were subjected to sorting CD4 T cells by using FACS Aria III, FACSAria or Fusion (BD).

Cell culture

$CD4^+$ T cells from spleens and/or lymph nodes of 6- to 12-week-old mice were purified by negative selection and magnetic separation (Miltenyi Biotec) followed by sorting of naive $CD4^+CD62L^+CD44^-CD25^-$ population using FACSAria III or FACSAria Fusion (BD). Naive $CD4^+$ T cells were activated by plate-bound anti-CD3 (10 μg/mL, Clone: 145-2C11) and anti-CD28 (10 μg/mL, 37.51) in media for 3 days with 5 different conditions. (1) Th17(β) cell-polarization with IL-6 (20 ng ml^{-1}, R&D Systems), human TGF-β1 (2.5 ng ml^{-1}, R&D Systems), anti-IFN-γ neutralizing antibodies (10 μg ml^{-1}, BioXCell), and anti-IL-4 neutralizing antibodies (10 μg ml^{-1}, BioXCell); (2) Th17(23) cell-polarization with IL-6 (20 ng ml^{-1}, R&D Systems), IL-23 (50 ng ml^{-1}, R&D Systems), anti-IFN-γ neutralizing antibodies (10 μg ml^{-1}, BioXCell), and anti-IL-4 neutralizing antibodies (10 μg ml^{-1}, BioXCell); (3) Th17 cell-full polarization with IL-6 (20 ng ml^{-1}, R&D Systems), IL-23 (50 ng ml^{-1}, R&D Systems), IL-1β (20 ng ml^{-1}, R&D Systems), human TGF-β1 (2.5 ng ml^{-1}, R&D Systems), anti-IL-2 neutralizing antibodies (10 μg ml^{-1}, BioXCell), anti-IFN-γ neutralizing antibodies (10 μg ml^{-1}, BioXCell), and anti-IL-4 neutralizing antibodies (10 μg ml^{-1}, BioXCell); (4) Th1 cell-polarization with IL-12 (20 ng ml^{-1}, R&D Systems) and anti-IL-4 neutralizing antibodies (10 μg ml^{-1}, BioXCell).; (5) iTreg cell-polarization with human TGF-β1 (2.5 ng ml^{-1}, R&D Systems), human IL-2 (100 IU ml^{-1}, National Cancer Institute), anti-IFN-γ neutralizing antibodies (10 μg ml^{-1}, BioXCell), and anti-IL-4 neutralizing antibodies (10 μg ml^{-1}, BioXCell).

Flow cytometry

Flow cytometry analysis and sorting was performed on a FACSVerse, FACSAria III, FACSAria Fusion (BD) or Cytek Aurora (Cytek Biosciences). Acquired data were analyzed with FlowJo software (TreeStar). For cell surface staining, the following anti–mouse antibodies were used: anti-CD4 (GK1.5 or RM4-5), anti-CD8 (53-6.7), anti-CD25 (PC61.5), anti-CD44 (IM7), anti-CD45.1 (A20), anti-CD45.2 (104), anti-CD45 (30-F11), anti-CD62L (MEL-14), anti-NKp46 (29A1.4), and anti-TCR-β (H57-597). For intracellular cytokine and transcription factor staining, cells were fixed and permeabilized with Foxp3 / Transcription Factor Staining Buffer Set (Thermo Fisher Scientific), and were stained with anti-RORγt (Q31-378), anti-T-bet (eBio4B10), anti-Foxp3 (FJK-16 s), anti-IL-17A (TC11-18H10.1 or eBio17B7), anti-IFN-γ (XMG1.2), and anti-c-Maf (sym0F1). Zombie NIR Fixable Viability kit (Biolegend) was used according to the manufacturer's protocol to exclude dead cells from analysis.

Library preparation for RNA Sequencing (small RNA-seq and mRNA-seq)

RNA-seq and small RNA-seq were performed and analyzed as described previously (Kuchen et al., 2010; Shih et al., 2016). Total RNA was prepared from approximately 1 million cells by using TRIzol or mirVana miRNA Isolation Kit (Thermo Fisher Scientific Inc.) and 200 ng or 1000 ng of total RNA were used to prepare libraries for RNA-seq (with TruSeq SR RNA sample prep kit (FC-122-1001, Illumina)) or small RNA-seq (with TruSeq Small RNA Sample Prep Kit (RS-200-0012, Illumina)) respectively by following manufacturer's protocol. The libraries were sequenced for 50 cycles (single read) with a HiSeq 2000 or HiSeq 2500 (Illumina).

Library preparation for Single cell RNA-sequencing (scRNA-seq)

For scRNA-seq analysis, Th cells were isolated from small intestinal lamina propria of *Il17a*$^{gfp/-}$ x *Mir221Mir222*$^{wt/Y}$ (IL17-GFP/WT) and *Il17a*$^{gfp/-}$ x *Mir221Mir222* $^{KO/Y}$ (IL17-GFP/miR-221/222-KO) male mice. Th17 cells (*Il17-gfp*+ $CD4^+$ $TCR\beta^+$ $CD44^+$ $CD62L^-$) were purified by FACS sorting by FACSAria III or FACSAria Fusion (BD) and scRNA-seq libraries were prepared by using Chromium Single Cell 3′ Reagent Kits v2 (10x Genomics) by following manufacturer's protocol. The libraries were sequenced on an Illumina HiSeq 3000 (Illumina, San Diego, CA).

Chromatin immunoprecipitation sequencing (ChIP-seq)

Cells cultured under indicated conditions were cross-linked for 10 min with 1% formaldehyde and harvested. Cells were lysed by sonication and immunoprecipitated with anti-H3K4me1 (ab8895, AbCam), anti-H3K4me3 (ab8580, AbCam), anti-H3K27me3 (07-449, Millipore), anti-STAT3 (14-6727, eBiosciences), and anti-p300 (sc-585, Santa Cruz Biotechnology) antibodies as previously described (Shih et al., 2016). Recovered DNA fragments were blunt-end ligated to the Illumina adaptors, amplified, and sequenced by using Genome Analyzer (Illumina, San Diego, CA).

RT-qPCR

Quantification of miRNA expression was performed as previously described (Takahashi et al., 2012). Total RNA was prepared by using TRIzol or mirVana miRNA Isolation Kit (Thermo Fisher Scientific). For reverse transcription and quantification of miRNA, TaqMan Reverse Transcription Kit was used in combination with TaqMan miRNA assays for snoRNA202 and hsa-miR-221 and −222 (Thermo Fisher Scientific Inc.). Results were properly normalized to snoRNA202 levels.

Luciferase assay

The vectors carrying 3′ UTR of *Maf* or *Il23r* cloned into a firefly/Renilla Duo-Luciferase reporter vector (pEZX-MT06) (GeneCopoeia) were transfected in HEK293T cells with miR-221/222 mimics or a control mimic (Dharmacon) by Lipofectamine LTX with Plus Reagent (Thermo Fisher Scientific). Firefly luciferase and Renilla luciferase activity were measured with Luc-Pair Duo-Luciferase Assay Kits 2.0 (GeneCopoeia).

DSS-induced colitis

Mice were received 2.0% dextran sulfate sodium salt (MW 36-50kD, 160110, MP Biomedicals) dissolved in sterile distilled water *ad libitum* for 7 days followed by regular drinking water for 3 days. Three sets of WT and miR-221/222 KO mice were tested; (1) *Mir221-Mir222* $^{fl/fl}$ mice (n = 4) and germline *Mir221Mir222* KO (n = 5); (2) *Mir221Mir222* $^{fl/fl}$ mice (n = 6) and *CD4-Cre Mir221Mir222* $^{fl/fl}$(n = 8); (3) *Rag2*-KO (n = 5) and *Rag2 Mir221Mir222 DKO* (n = 6)

Histology

Isolated small intestines from *Mir221Mir222* $^{fl/fl}$ or *Mir22Mir/222* KO were flushed with ice cold PBS and divided into sections corresponding to duodenum, jejunum and ileum. Each section was opened longitudinally, then rolled into a 'Swiss roll', fixed with 10% neutral formalin solution. Samples were processed for paraffin sections and stained with H&E or periodic acid-Schiff (PAS) at Histoserv (Germantown, MD). Intestines were evaluated by an investigator with experimental conditions masked, using the following criteria; 0: no visible infiltrate; 0.5: infiltrate in < 10% of sections; 1: infiltrate in < 25% of sections; 1.5: infiltrate in < 35% of sections; 2: infiltrate in < 50% of sections.

Microbiome analysis

Microbiota composition of feces was determined by 16S rRNA analysis (ZymoBIOMICS Services) as briefly described in the followings. DNA was extracted from fecal samples stabilized in DNA/RNA Shield (Zymo Research, CA, US) with ZR Fecal DNA Miniprep (Zymo Research) according to the manufacturer's protocol. Bacterial 16S ribosomal RNA gene targeted sequencing was performed as previously described with slight modification (Kozich et al., 2013). The general Bacterial 16S primers, 341f (CCTACGGGNGGCWGCAG) and 805r (GACTACHVGGGTATCTAATCC), were used to amplify the v3-4 region of the 16S rRNA gene. PCR amplicons were purified using Select-a-Size DNA Clean & Concentrator (Zymo Research). The 16S rRNA was sequenced using Illumina MiSeq with v2 reagent kit (500 cycles, with 10% PhiX mix, and in paired-end mode). Reference sequences were obtained from the workflow of pick_open_reference_otus.py using SILVA (v. 123) (Quast et al., 2013). Taxa that have an abundance significantly different among groups were identified by LEfSe with default settings ($p > 0.05$ and LDA effect size > 2) (Segata et al., 2011).

QUANTIFICATION AND STATISTICAL ANALYSIS

mRNA-seq analysis

Raw sequencing data were processed with CASAVA 1.8.2 to generate FastQ files. Sequence reads for RNA-seq were mapped onto the mouse genome build mm9 using TopHat 2.1.0. Gene expression values (FPKM, fragments per kilobase exon per million mapped reads) were calculated with Cufflinks 2.2.1. (''Differential gene and transcript expression analysis of RNA-seq experiments with TopHat and Cufflinks.,'' 2012)).

microRNA-seq analysis

For small RNA-seq, 5′ 19 base sequence reads were mapped onto mm9 with Bowtie (0.12.8) (Langmead et al., 2009), allowing no mismatch. Gene expression values (RPKM, reads per kilobase exon per million mapped reads) were calculated by Partek Genomics Suite (6.6/6.14.0514). BigWig tracks were generated from Bam files and converted into Bedgraph format using BEDTOOL. These were further reformatted with the UCSC tool bedGraphToBigWig. We used genes that are included in consensus coding sequences set (released: 8/27/2017)(The consensus coding sequence (CCDS) project: Identifying a common protein-coding gene set for the

human and mouse genomes) and are expressed over 10 FPKM in at least one condition. The differential gene expression was calculated by Partek Genomics Suite (6.6/6.14.0514).

scRNA-seq analysis

10x Genomics CellRanger and Illumina Bcl2fastq software were used to demultiplex and generate FastQ files. CellRanger and STAR were used to align to mouse mm10 genome. CellRanger was used to generate counts and output matrix files were loaded into R for analysis using the Seurat 3.1.5 package. Low-quality cells were filtered out based on > 5% mitochondrial gene expression and number of genes per cell < 200 or > 2500. Data were integrated, normalized, and transformed for downstream analysis. Cells were clustered using Seurat's graph-based clustering and visualized using UMAP. Gene expression was subsequently determined in each cluster. Data were visualized using ggplot2 3.3.0.

ChIP-seq analysis

We aligned ChIP-seq reads to the mouse genome (build mm9) with Bowtie (v0.12.8) (Langmead et al., 2009), allowing two mismatches. We then identified peaks using MACS (v 1.4.3; default p value threshold of 1E-5) (Zhang et al., 2008). We visualized each ChIP-seq dataset by counting positional coverage across the genome (BEDTOOLS v2.24) (Quinlan and Hall, 2010), reformatting to bigWig (bedGraphToBigWig), and viewing in IGV (Thorvaldsdóttir et al., 2013).

Gene Set Enrichment Analysis (GSEA)

GSEA from the Massachusetts Institute of Technology (https://www.broad.mit.edu/gsea) was used. For analyzing *in vivo* Th cells derived from bone marrow chimera experiment, we first extracted gene signatures from public data for the followings; (1) Th17 (Ciofani et al., 2012), (2) human IL-10+ Th17 (Aschenbrenner et al., 2018), (3) human IL-10- Th17 (Aschenbrenner et al., 2018), (4) c-Maf-induced (Ciofani et al., 2012), (5) Th2 (Ranzani et al., 2015) (also see Table S2), then run GSEA analyses for enrichment against gene expression profiles of WT and miR-221/222 KO gut $CD4^+$ T cells (Figures 5F and S5A).

Statistics

For calculation of comparison between groups, unpaired t test was used. Values about WT and miR-221/222 KO $CD4^+$ T cells within each mouse were compared using the paired t test (Figure 4C, D, and S4). P values and Log2 fold change (Log2 ((mean WT FPKM)+1)/((mean KO FPKM)+1)) was projected to a volcano plot (Fig.S4). In all bar graphs, error bars represent SEM. Statistical analysis was performed using the Prism software (GraphPad). *P value*s less than 0.05 were considered significantly different.